Chapter 14

Subsurface Pressures from Drill-Stem Tests, Uinta and Piceance Basins, Utah and Colorado

Click here to return to
Volume Title Page

By Philip H. Nelson

Chapter 14 *of*

Petroleum Systems and Geologic Assessment of Oil and Gas in the Uinta-Piceance Province, Utah and Colorado

By USGS Uinta-Piceance Assessment Team

U.S. Geological Survey Digital Data Series DDS–69–B

U.S. Department of the Interior
U.S. Geological Survey

U.S. Department of the Interior
Gale A. Norton, Secretary

U.S. Geological Survey
Charles G. Groat, Director

Version 1.0 2003

For sale by U.S. Geological Survey, Information Services
Box 25286, Denver Federal Center
Denver, CO 80225

Published in the Central Region, Denver, Colorado
Manuscript approved for publication July 24, 2002

ISBN=0-607-99359-6

Contents

Figures

Table

Subsurface Pressures from Drill-Stem Tests, Uinta and Piceance Basins, Utah and Colorado

By Philip H. Nelson

Abstract

Pressure data from oil and gas wells within the Uinta Basin, Utah, and the Piceance Basin, Colorado, have been compiled from shut-in pressures obtained from drill-stem tests. Tests in wells completed prior to 1985 include 2,019 pressure measurements from the Uinta Basin and 450 pressure measurements from the Piceance Basin. However, the number of useful pressure measurements is considerably less, because many drill-stem tests fail to stabilize at the actual formation pressure if the permeability is low. By excerpting the maximum pressures recorded in a collection of wells within an area, the trend of formation pressure within that area can be approximated.

Areal compilations of pressures from drill-stem tests show that overpressured rock formations occur throughout much of the northern and eastern areas of the Uinta Basin. In particular, significant overpressuring (0.5<pressure gradient<0.8 psi/ft) is found throughout much of the Altamont-Bluebell field at depths ranging from 10,000 to 13,000 feet, equivalent to 5,000–8,000 feet below sea level. Limited data indicate that the pressure gradient declines at depths greater than 13,000 feet. Throughout the eastern Uinta Basin, moderate overpressuring (0.46<pressure gradient<0.5 psi/ft) occurs commonly, with local evidence of significant overpressured zones, but pressure gradients greater than 0.6 psi/ft are rare. Pressure data from drill-stem tests measured in the Piceance Basin are not as diagnostic as in the Uinta Basin, due to lower spatial density of pressure tests and evidence that pressures measured in Cretaceous rocks of the Piceance Basin are not representative of actual formation pressure.

Introduction

Geologists are well aware of the relevance of abnormal pressure to hydrocarbon accumulations in the Uinta and Piceance Basins (Lucas and Drexler, 1976; Johnson, 1989b; Wilson and others, 1998). As Law and Spencer (1998, p. 2) have noted, "***(knowledge of) the large number of abnormally pressured areas in the Rocky Mountain region of the United States is a consequence of several detailed investigations of abnormally pressured, unconventional gas reservoirs. In this region and elsewhere in North America, investigators have noted the close association of hydrocarbon accumulations, particularly unconventional gas accumulations, and abnormal pressures." Much of the oil and gas in the Uinta and Piceance Basins occurs in basin-centered (continuous) systems. Consequently, knowledge of abnormal pressuring in these basins is of especial interest, because basin-centered gas accumulations are nearly always associated with abnormal pressures (Law and Spencer, 1998).

Although the need for accurate determinations of formation pressure in the characterization of basin-centered reservoirs is well established, the determination of formation pressure itself is anything but straightforward. Holm (1998) ranked the methods of obtaining formation pressure in the following order: repeat formation tester, drill-stem tests, mud-weight data, and pressure kicks. Drill-stem tests (DSTs), which are the subject of this report, measure the downhole pressure of fluid within the wellbore, rather than the formation pressure itself. DST results must be extrapolated and corrected carefully in order to obtain the best estimate of true formation pressure (Holm, 1998). No such analyses were carried out in this study, which simply presents the unanalyzed pressure data from a large number of DSTs within the Uinta and Piceance Basins. It is believed that the bias imposed by this lack of detailed analysis underestimates the formation pressure in a certain fraction of cases, as discussed below. As a reminder of this bias, a measurement is described as *apparent pressure* or *apparent pressure gradient*.

The DST pressure data are presented in compact graphs arrayed in map-like format ("checkerboard plots") and in conventional plots of pressure versus depth. The pressure data have not been integrated with stratigraphy or indicators of thermal maturity; the analysis is limited to comments on the validity of the data and the distribution of overpressured conditions. The results appear most informative in the Altamont-Bluebell field of the Uinta Basin, moderately informative in the eastern Uinta Basin, and rather disappointing in the Piceance Basin. Before a discussion of the pressure data, nomenclature and sources of data are presented in the next section.

Definitions and Plotting Methods

A common method of plotting fluid pressure as a function of depth is illustrated in figure 1*A*. In this hypothetical example, true reservoir pressure increases hydrostatically to a depth of 5,000 ft and then increases more rapidly with depth, reaching a value of 5,580 psi at 9,000 ft. This pressure is equivalent to a *nominal* pressure gradient of 0.62 psi/ft, where the nominal pressure gradient is equal to the measured pressure divided by the depth. Three values of nominal pressure gradient are illustrated by the dashed blue lines. Notice that the *local* pressure gradient, shown as the solid green line connecting the pressure values at 8,000 and 9,000 ft, is considerably greater than the nominal gradient. Fluid flow in the subsurface is driven by the local pressure gradient, but the nominal pressure gradient is commonly cited because it provides a convenient normalization for pressures measured at different depths. Alternative methods of plotting pressure data are illustrated in figures 1*B* and 1*C*. The compact display of pressure gradient versus depth (fig. 1*B*) is used in figures 5, 11, and 12. The higher resolution of a differential pressure plot (fig. 1*C*) shows the details of pressure excursions and is used in figure 8.

The hydrostatic gradient is commonly referenced to the weight of fresh water. A column of water 1 ft (12 in.) high with an area of 1 in.^{2} contains $2.54^3 \times 12 = 196.64$ cm^3. At standard temperature and pressure, this volume holds 196.64 g of fresh water, equivalent to a weight of 196.64 g / 453.59 g/lb=0.433 lb, thereby establishing the fresh-water hydrostatic gradient of 0.433 psi/ft. In terms of the units used for mud weight, the equivalent density is 1.0 g/cm^{3}x3,785.4 cm^3/gal÷453.59 g/lb, or 8.345 lb/gal. In the hypothetical example of figure 1, the actual pressure increases in accordance with the hydrostatic gradient from 0 to 5,000 ft.

It is difficult to measure the actual pressure in low-permeability formations, particularly if the formation adjacent to the wellbore is invaded by drilling fluids or otherwise damaged by the drilling process. As a result, the measured (apparent) pressure, represented by open circles in figure 1*A*, is sometimes less than the true (actual) formation pressure, represented by red triangles. Also, the apparent pressure gradient is less than the actual pressure gradient (fig. 1*B*).

The actual hydrostatic gradient varies with temperature, pressure (depth), and salinity, all of which affect the density of water. Density increases linearly with salt content, decreases nonlinearly with temperature, and increases slightly with pressure (Collins, 1992). When considering variations on the scale of 1,000 vertical feet in the subsurface, water density variations are largely due to variations in salinity, because temperature and pressure both increase with depth and their effects upon density are somewhat compensating. The salinity of water samples from the Altamont-Bluebell field rarely exceeds that of sea water, which is nominally 32,000 ppm. As an example, at a depth of 8,000 ft, a temperature of 120°F, and a total dissolved solids of 32,000 ppm, the density of water is 1.027 g/cm^3, resulting in a *local* hydrostatic gradient of 0.444 psi/ft. The *nominal* hydrostatic gradient (reservoir pressure divided by depth) would be a value between 0.433 and 0.444 psi/ft, depending upon salinity and temperature variations with depth.

Formation pressures less than hydrostatic (0.433 psi/ft) are referred to as *underpressure.* Underpressured zones are much more difficult to identify than overpressured zones, so consequently more overpressured systems have been identified than underpressured systems (Law and Spencer, 1998). The difficulty arises because measurements which fail to reach actual formation pressure cannot be readily distinguished from valid measurements of formation pressures that are truly less than hydrostatic. The only criterion left, then, is one of spatial homogeneity. If pressure data less than hydrostatic are intermingled with pressure data that are at hydrostatic pressure or greater, then it is unlikely that an underpressured zone has been detected. Conversely, if all readings in a depth range from a cluster of wells are below hydrostatic, then it is probable that an underpressured zone exists. In this report, evidence has been found for underpressuring in the shallow part of the Altamont-Bluebell field.

Pressure in excess of hydrostatic is referred to as *overpressure*, but because hydrostatic pressure varies with hydrologic conditions, no single threshold value can be adopted to define overpressure. Spencer (1987) considered reservoirs to be significantly overpressured if the pressure gradient exceeds 0.50 psi/ft in basins with fresh to moderately saline water and 0.55 psi/ft in basins with very saline water. Clearly, the commencement of overpressuring begins at values less than 0.5 psi/ft in basins with moderately saline water. However, a single criterion is not as important as the patterns of pressure behavior with depth in a single well and laterally between wells. In this report, zones with pressure gradients between 0.46 and 0.50 psi/ft are referred to as *moderately overpressured* and zones with gradients greater than 0.50 psi/ft as *significantly overpressured*. A value of 0.46 psi/ft, which is slightly greater than the expected range for the Altamont-Bluebell field, is used as a single visual threshold for overpressure on plots of pressure gradient (figs. 5, 11, 12). On pressure plots such as figure 1*A*, lines of varying gradients are shown.

Sources of Data

The primary source of data presented in this report is a previously unpublished compilation of DST pressures initiated by C.W. Spencer of the U.S. Geological Survey. Initial and final shut-in pressures from DSTs were compared, and the greater of the two was selected and is referred to in this report as the *apparent pressure*. The apparent pressure divided by the depth is the *apparent pressure gradient* in psi/ft. The modifier “apparent” is used to emphasize that, without further analysis, the unextrapolated pressure recovered from a DST record is apt to be less than the actual reservoir pressure (Spencer, 1994).

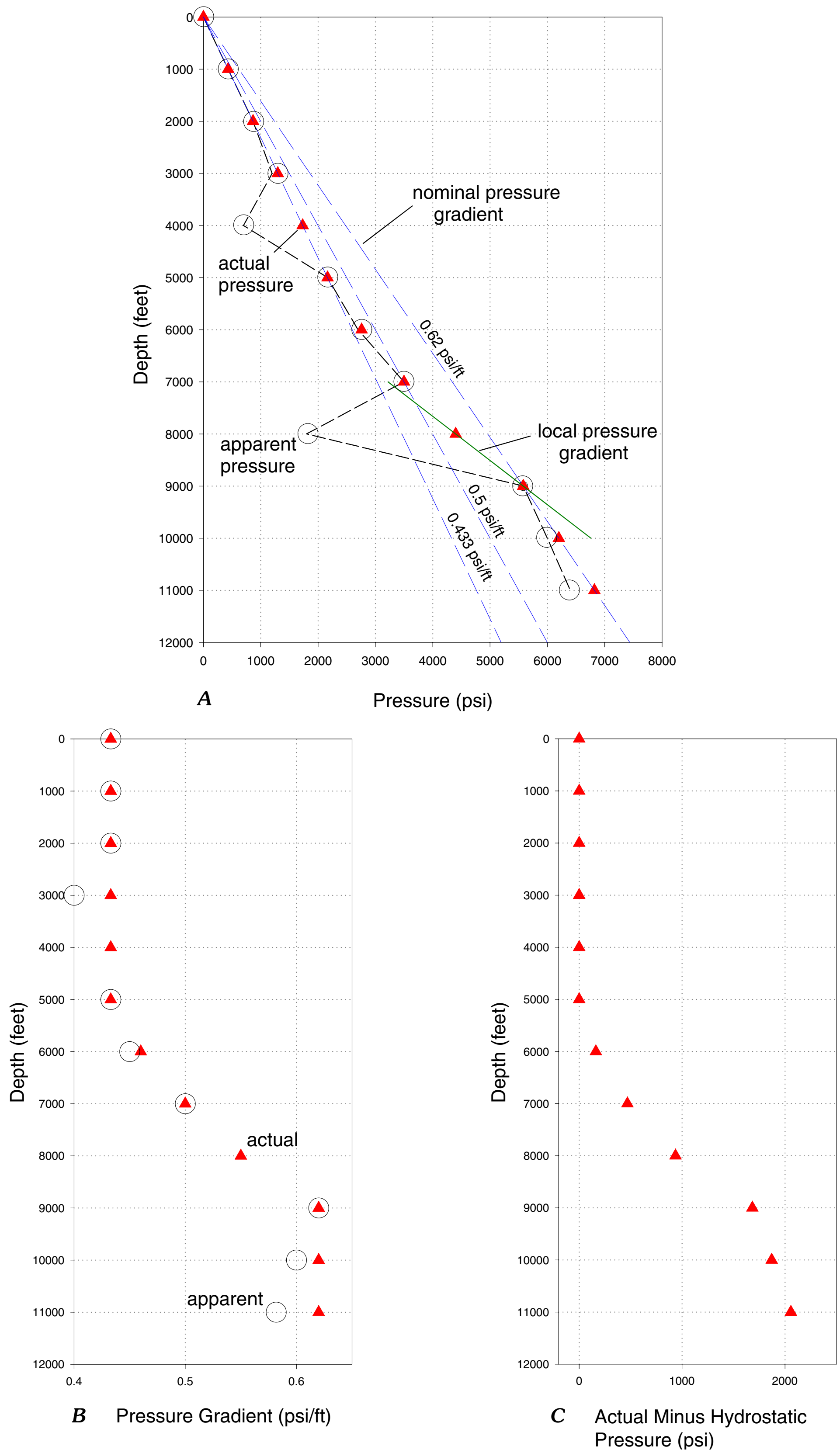

Figure 1. Three methods of displaying pressure data as a function of depth, using hypothetical pressure values. *A*, "Actual" (hypothetical true) reservoir pressure (red triangles) and "apparent" (hypothetical measurements) pressure (open circles) as function of depth. Apparent pressures are less than actual pressures. *B*, Actual and apparent nominal pressure gradients. *C*, Actual minus hydrostatic pressure, where hydrostatic pressure in psi equals 0.433 times the depth in feet.

The well locations in which DSTs were run are shown in figures 2 and 3. The apparent pressure gradients are shown as histograms, presented by basin and by geologic age, in figure 4. The histograms show the number of measurements examined in this study. The histograms of figure 4 also demonstrate that many measurements lie well below the lowest pressure that might be conceived as underpressure, and that only a small fraction of total measurements reach values which can be described as overpressure. It is this small fraction of measurements that are significant in examining the hydrocarbon production potential of sedimentary basins (Spencer, 1994).

A second, smaller set of DST data was compiled by Wesley and others (1990). Using a standard method of analyzing DST records called the Horner method, Wesley and others (1990) obtained 78 extrapolated (static) reservoir pressures and pressure gradients from 50 DSTs (some tests utilized two or three pressure gauges). The tests were conducted in 16 wells distributed among 11 townships within the Uinta Basin. The pressure values obtained by the Horner method should be close to the *actual reservoir pressure*, hence the pressure gradient values obtained by Wesley and others are referred to herein as the *actual pressure gradient*.

The actual pressure gradients compiled by Wesley and others (1990) provide a check on the (more voluminous) apparent pressure gradients compiled by Spencer. Of the 50 DSTs analyzed by Wesley and others, 34 were also in the Spencer data set. Of these 34 pressure gradients, 20 fell within 0.015 psi/ft of their counterparts, whereas 11 values analyzed by Wesley and others were greater than their counterparts by more than 0.015 psi/ft (that is, the "actual" values were greater than the "apparent" values). In three tests, the values determined to be the actual pressure gradient, as analyzed by Wesley and others, were less than the apparent pressure gradient. In other words, the apparent pressure gradient was equal to the actual pressure gradient to within ±0.015 psi/ft in 59 percent of the tests, was inexplicably greater than the actual value in 9 percent of the tests, and was less than the actual value in 32 percent of the tests. Considering the 11 tests (32 percent) in which actual values exceeded apparent ones, and excluding one test zone that registered a pressure gradient above lithostatic, the actual values exceeded the apparent values by a range of 0.02–0.15 psi/ft, with an average of 0.06 psi/ft. No corrections were made to the Spencer data set, which is used throughout this report. One should bear in mind that about one-third of the apparent pressure gradient values displayed in this report are likely to be less than the actual pressure gradient.

The data presented in this report are taken from the Spencer data set, with the single addition of pressure data from the CER MWX-1 well in the Piceance Basin (chapter 15 by Nelson, this CD-ROM). The pressure data from MWX-1 were obtained from well tests through perforations, not from DSTs.

Uinta Basin

Apparent pressure gradient data for the Uinta Basin are shown in the "checkerboard plot" of figure 5. In order to present the data in the compressed format of figure 5, the nominal pressure gradient defined in figure 1*B* is plotted instead of pressure. Each square in the plot contains all pressure gradients determined within a 6×6-mi township. The squares are arranged in a grid that approximates the physical location of the townships; locations of townships and wells are shown in figure 2.

Within each square plot, a horizontal solid blue line serves as the 10,000-ft depth reference. In some of the township squares, a horizontal dashed magenta line shows the depth of the Tertiary Long Point Bed of the Green River Formation as defined by Johnson (1989a). The Long Point Bed was deposited during a major expansion of Eocene Lake Uinta. It separates fluvial-dominated deposits below from overlying lacustrine deposits.

The DST data of figure 5 show evidence for overpressured reservoirs throughout much of the northern and eastern parts of the Uinta Basin. Although few tests were run in the southwestern part of the basin, there is local evidence of overpressuring. In the following sections of this report, the pressures in the oil-producing Altamont-Bluebell field and in the gas-producing eastern part of the basin will be examined more closely.

Altamont-Bluebell Field, Uinta Basin

As a basin-centered (continuous) oil accumulation, the Altamont-Bluebell field is fairly unique. Its association with abnormal formation pressures also is unusual, as pointed out by Law and Spencer (1998, p. 7): "Curiously, the fluid phase of nearly all abnormally pressured hydrocarbon accumulations is gas. Notable exceptions include the Paleocene and Eocene Wasatch, Colton, and Green River Formations in the Uinta Basin of Utah."

Pressure data from DSTs are plotted as a function of depth (fig. 6*A*–*J*) for 52 wells in 10 areas within the Altamont-Bluebell field in the Uinta Basin. Lines of constant pressure gradient are also shown on the figures. Many pressure readings are less than the pressure required for a nominal hydrostatic gradient of 0.433 psi/ft. Most of these readings are believed to be unrepresentative of true reservoir pressure due to inadequate pressure buildup during the test. All 10 plots show pressures that can be characterized as overpressure, that is, having a nominal pressure gradient greater than 0.46 psi/ft. Pressures are high enough at some depth in 7 of the 10 areas

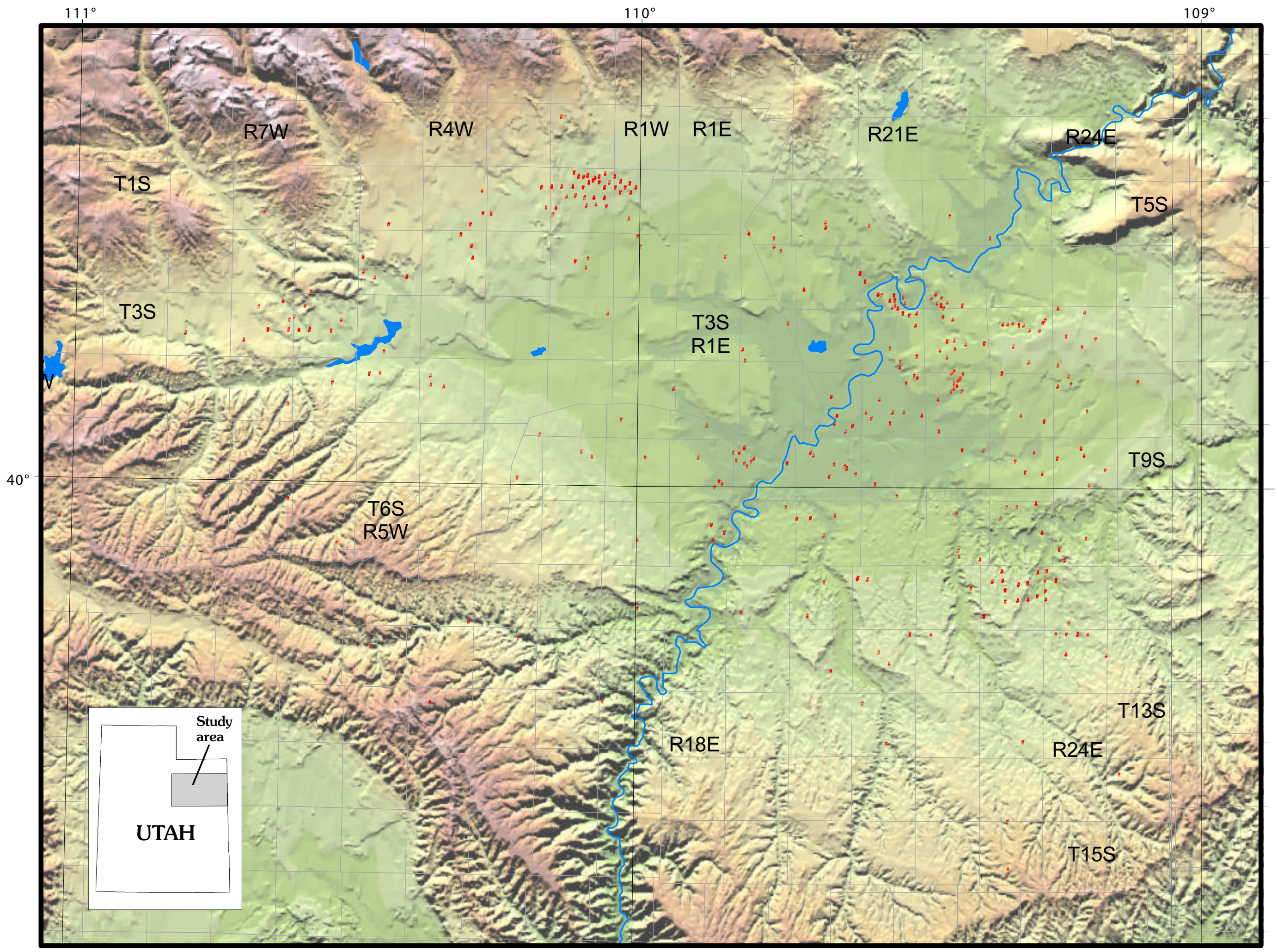

Figure 2. Well locations (red dots) in Uinta Basin, Utah. The Green River runs from northeast to southwest across the area. The boundary between two systems of township and range coordinates wanders through the center of the map, offsetting the two grids. Well locations are plotted at USGS quarter-mile data cell center points. All wells were completed prior to 1985 and lie within the boundary of the area assessed for oil and gas potential by the USGS.

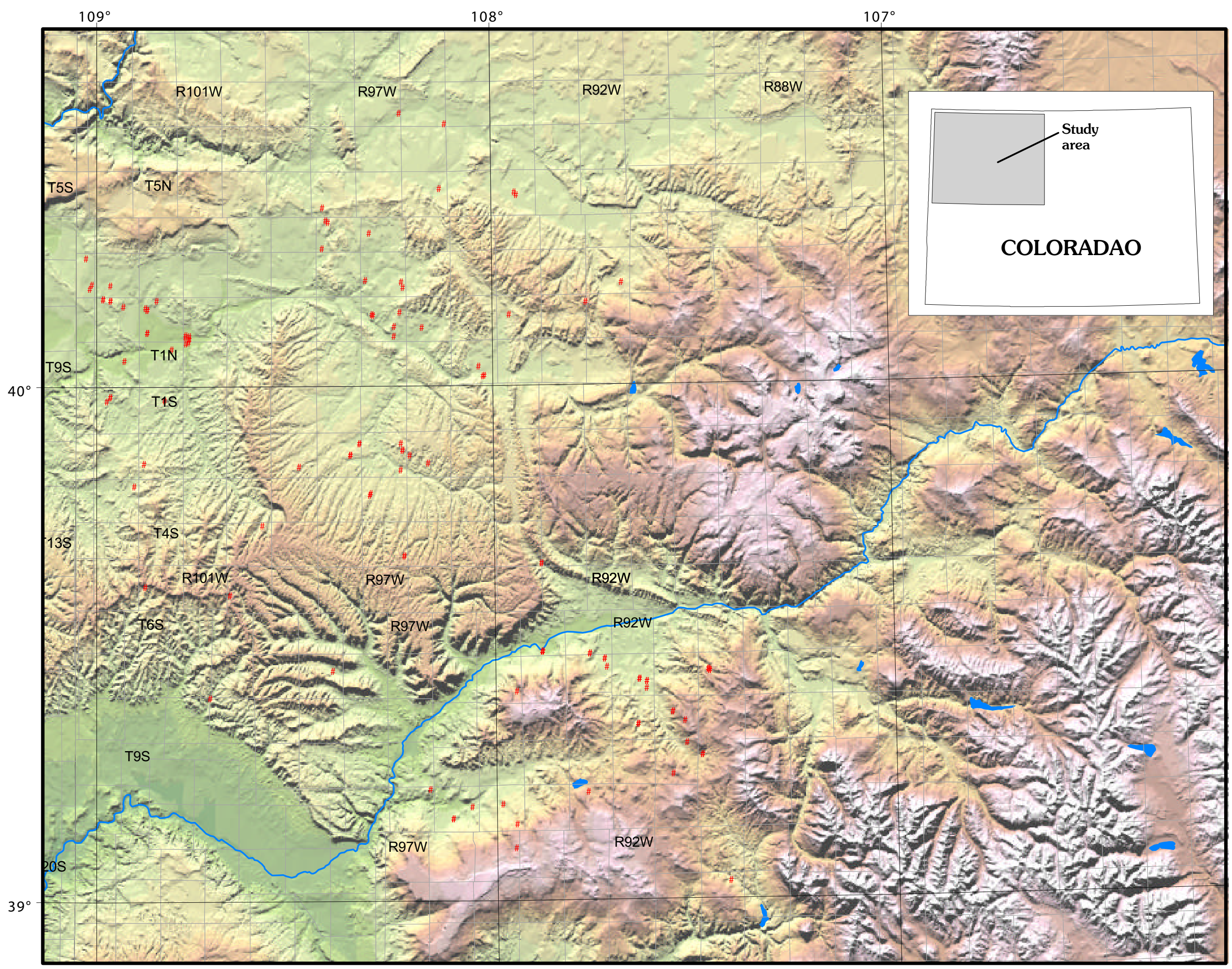

Figure 3. Well locations (red dots) in Piceance Basin, Colorado. The Colorado River runs from east to southwest across the area. The State line between Utah and Colorado lies immediately west of long 109° W. Well locations are plotted at USGS quarter-mile data cell center points. All wells were completed prior to 1985 and lie within the boundary of the area assessed for oil and gas potential by the USGS.

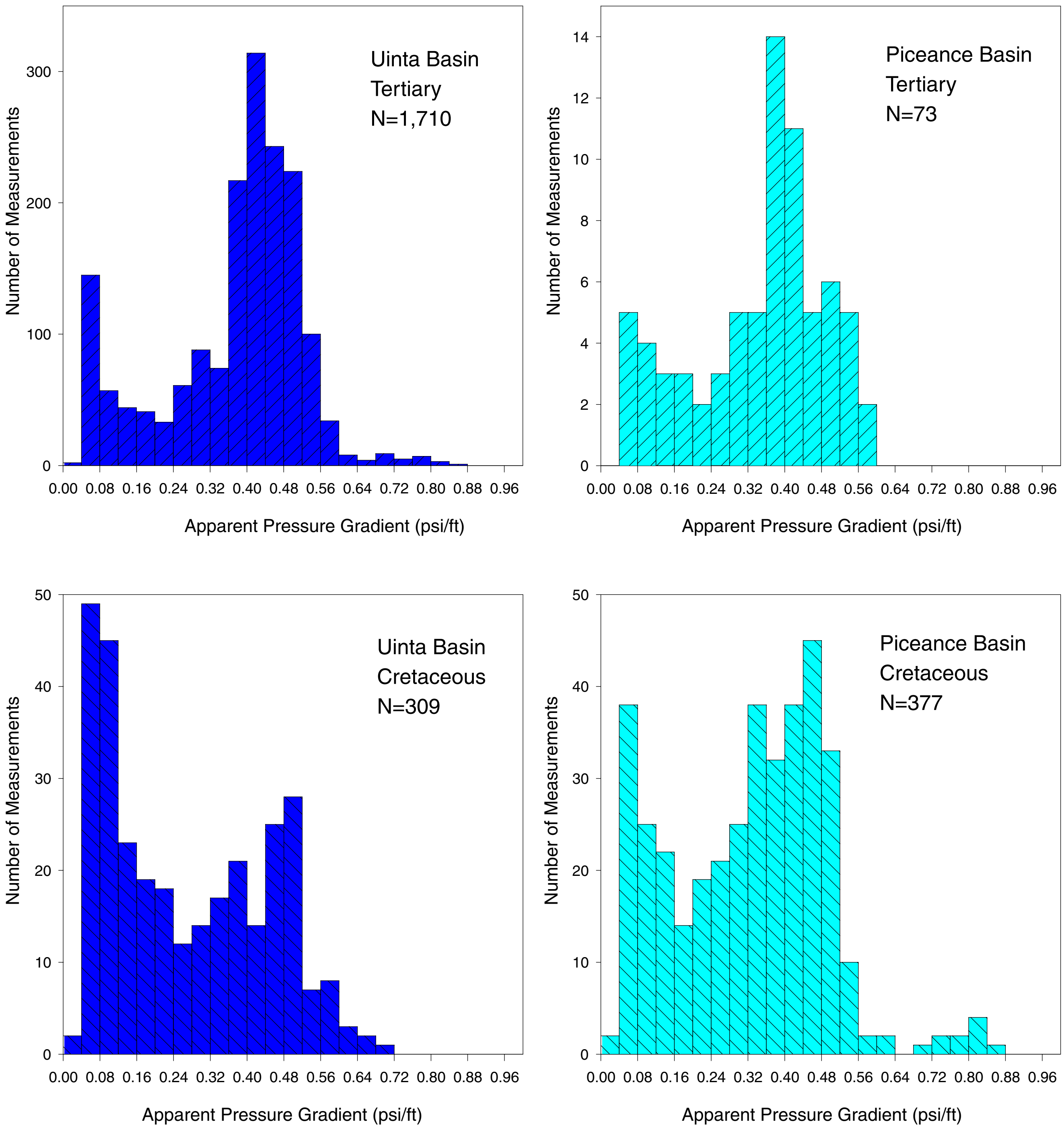

Figure 4. Apparent pressure gradient (psi/ft) in Uinta and Piceance Basins. N=total number of measurements.

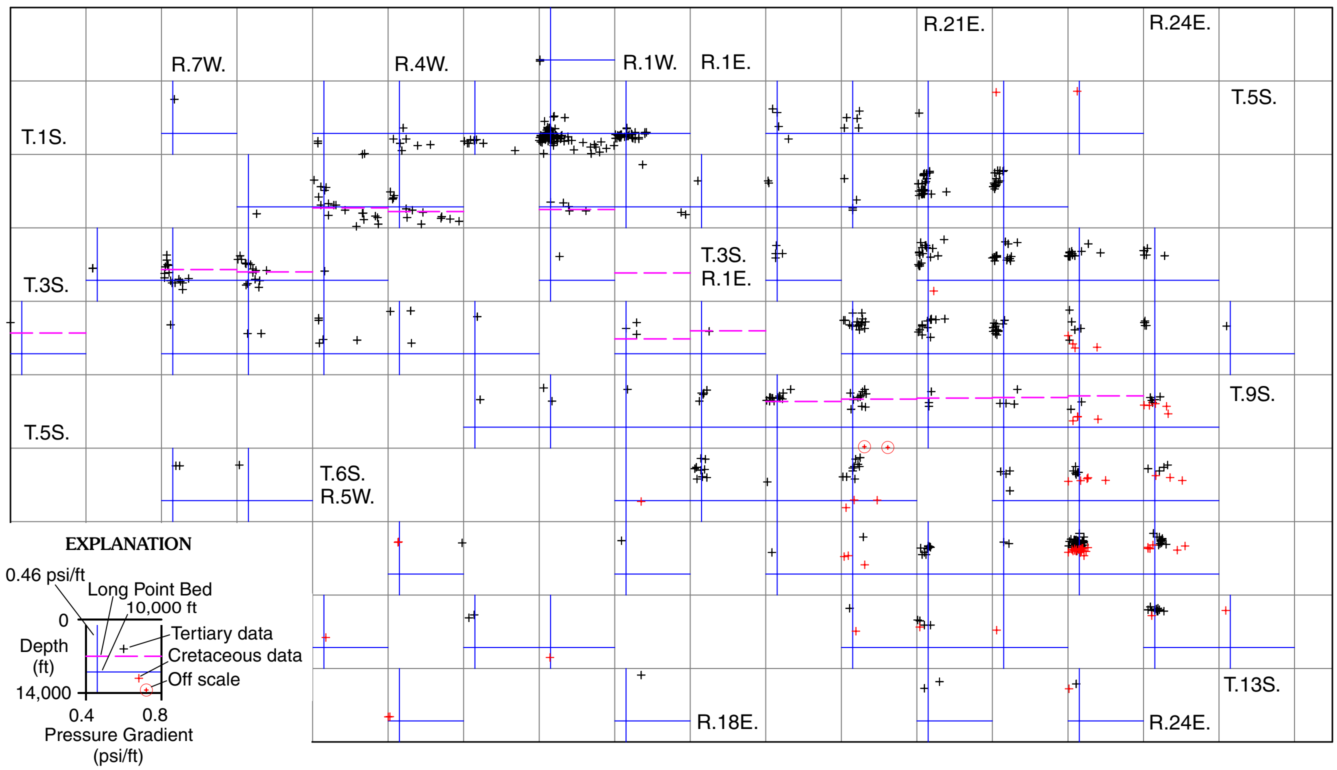

Figure 5. Apparent pressure gradient as a function of depth in Uinta Basin. Each square shows all drill-stem tests within a township recording an apparent pressure gradient greater than 0.4 psi/ft. Within a square, pressure gradients range from 0.4 to 0.8 psi/ft and depth ranges from 0 to 14,000 ft below surface. Tertiary data (black +) and Cretaceous data (red +) sometimes intermingle because the depth of the Cretaceous-Tertiary boundary varies within a township. Two circled points in R. 20 E., T. 9 S. represent measurements at 15,709 and 14,666 ft with pressure gradients of 0.522 and 0.646 psi/ft. Vertical blue line shows a reference gradient of 0.46 psi/ft and horizontal blue line shows a depth reference of 10,000 ft. Horizontal magenta line shows depth of Tertiary Long Point Bed, taken from Johnson (1989a). Township and range conventions change near the center of the plot. Locations shown here are only approximate; see figure 2 for exact locations of townships.

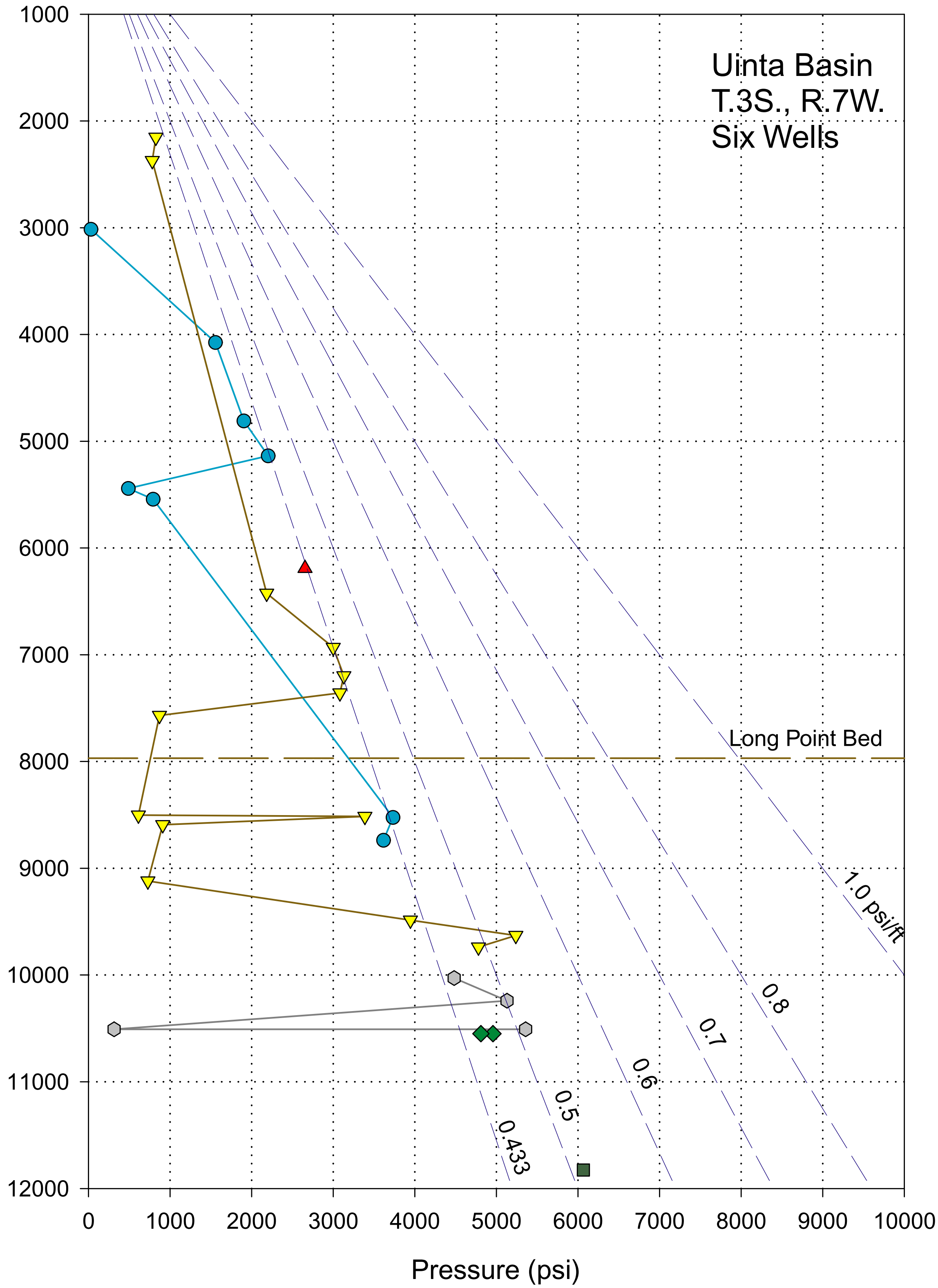

Figure 6*A*. Pressure as function of depth in T. 3 S., R. 7 W. in Altamont-Bluebell field of Uinta Basin. Each symbol represents the pressure from one drill-stem test; connected symbols show data from one well. Dashed lines show constant pressure gradient ranging from hydrostatic (0.433 psi/ft) to lithostatic (1.0 psi/ft). Depth of Long Point Bed from Johnson (1989a).

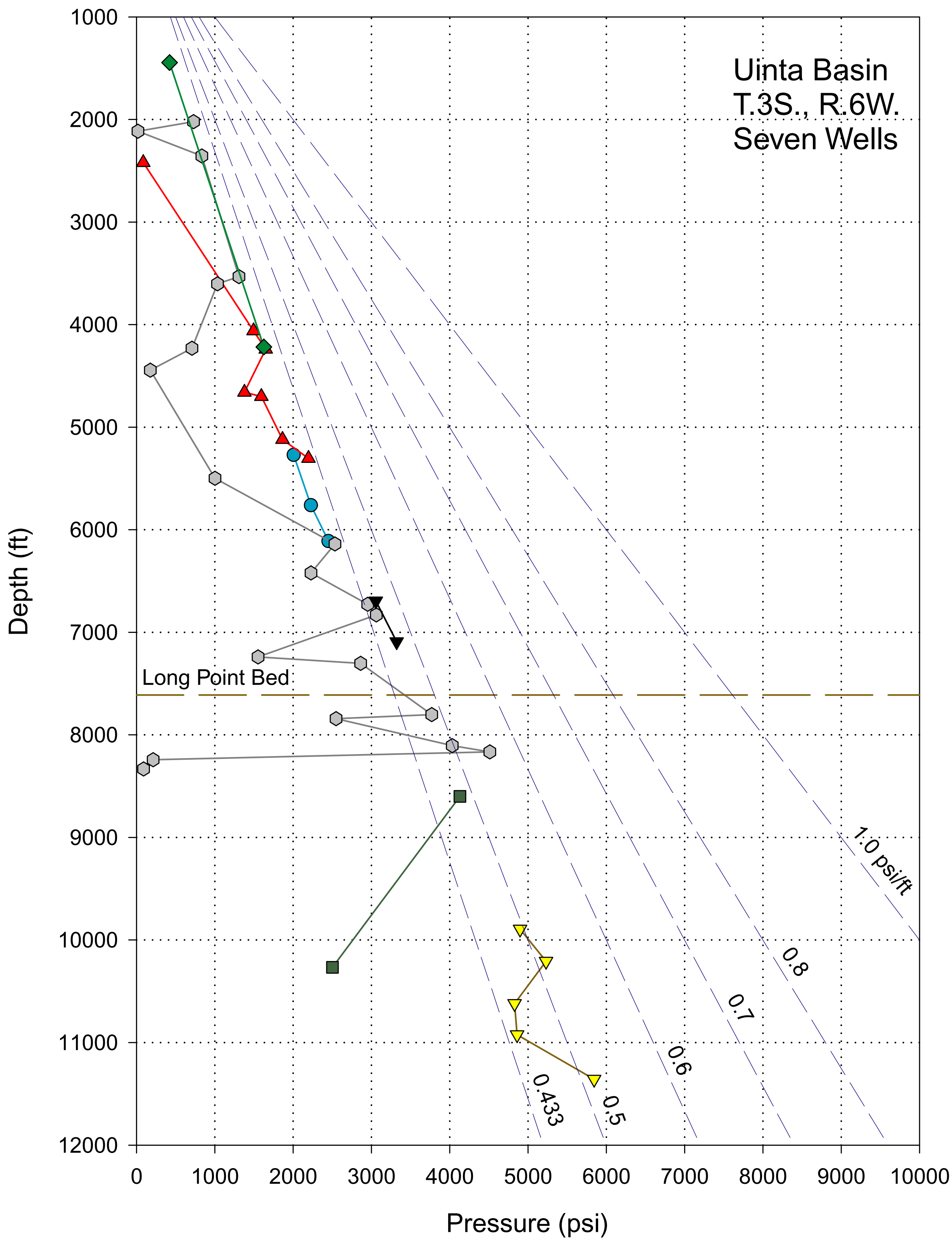

Figure 6*B*. Pressure as function of depth in T. 3 S., R. 6 W. in Altamont-Bluebell field of Uinta Basin. Each symbol represents the pressure from one drill-stem test; connected symbols show data from one well. Dashed lines show constant pressure gradient ranging from hydrostatic (0.433 psi/ft) to lithostatic (1.0 psi/ft). Depth of Long Point Bed from Johnson (1989a).

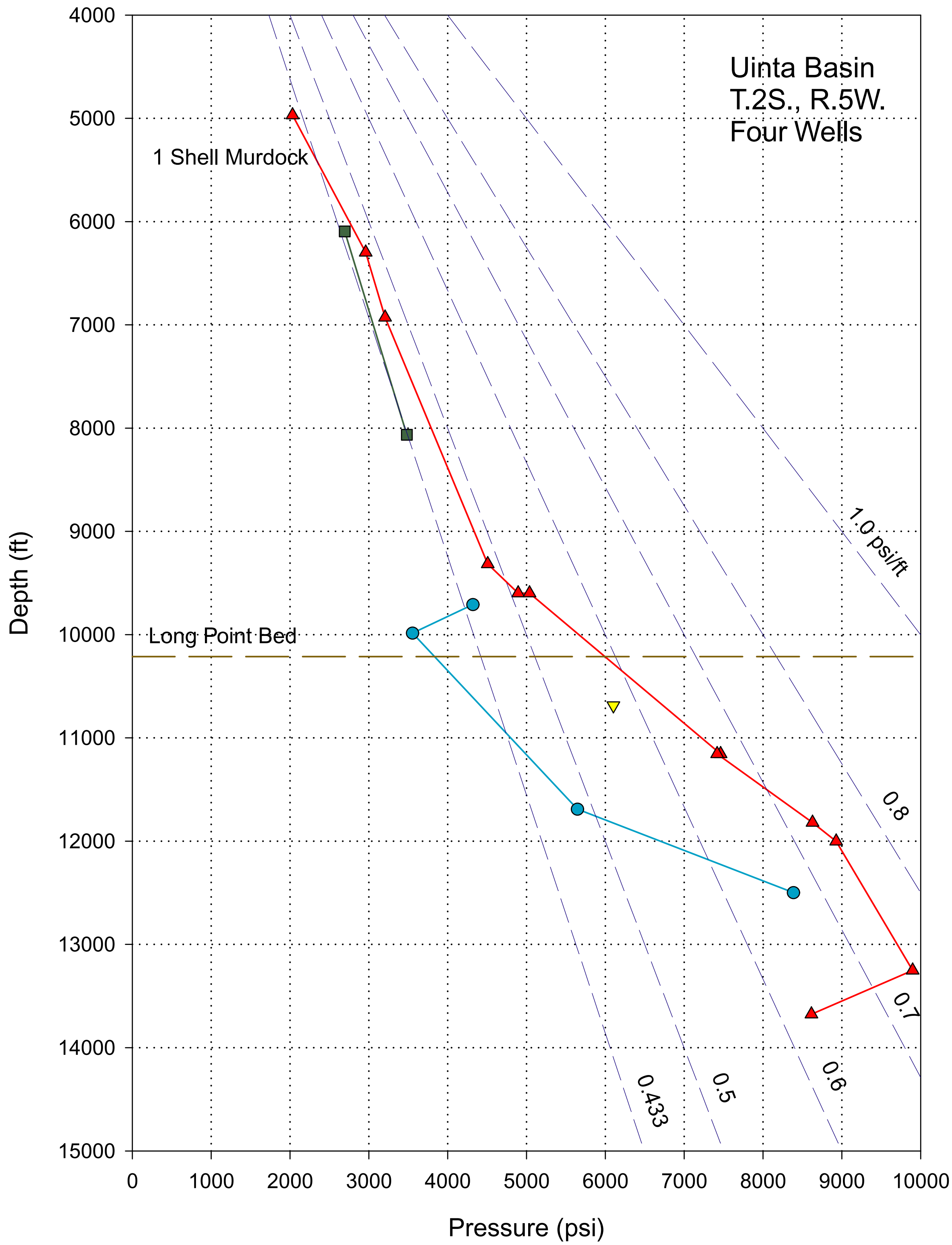

Figure 6*C*. Pressure as function of depth in T. 2 S., R. 5 W. in Altamont-Bluebell field of Uinta Basin. Each symbol represents the pressure from one drill-stem test; connected symbols show data from one well. Dashed lines show constant pressure gradient ranging from hydrostatic (0.433 psi/ft) to lithostatic (1.0 psi/ft). Depth of Long Point Bed from Johnson (1989a).

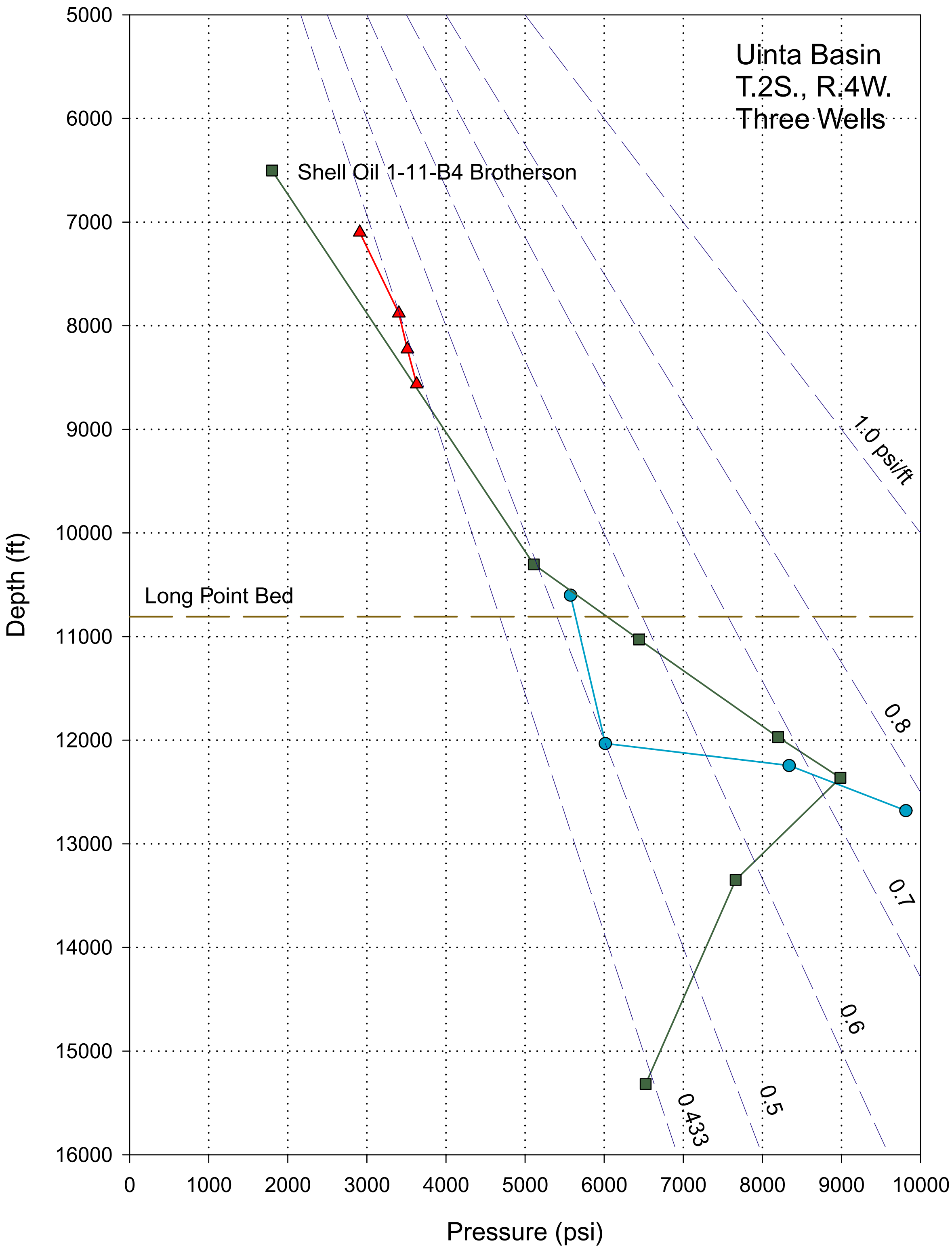

Figure 6*D*. Pressure as function of depth in T. 2 S., R. 4 W. in Altamont-Bluebell field of Uinta Basin. Each symbol represents the pressure from one drill-stem test; connected symbols show data from one well. Dashed lines show constant pressure gradient ranging from hydrostatic (0.433 psi/ft) to lithostatic (1.0 psi/ft). Depth of Long Point Bed from Johnson (1989a).

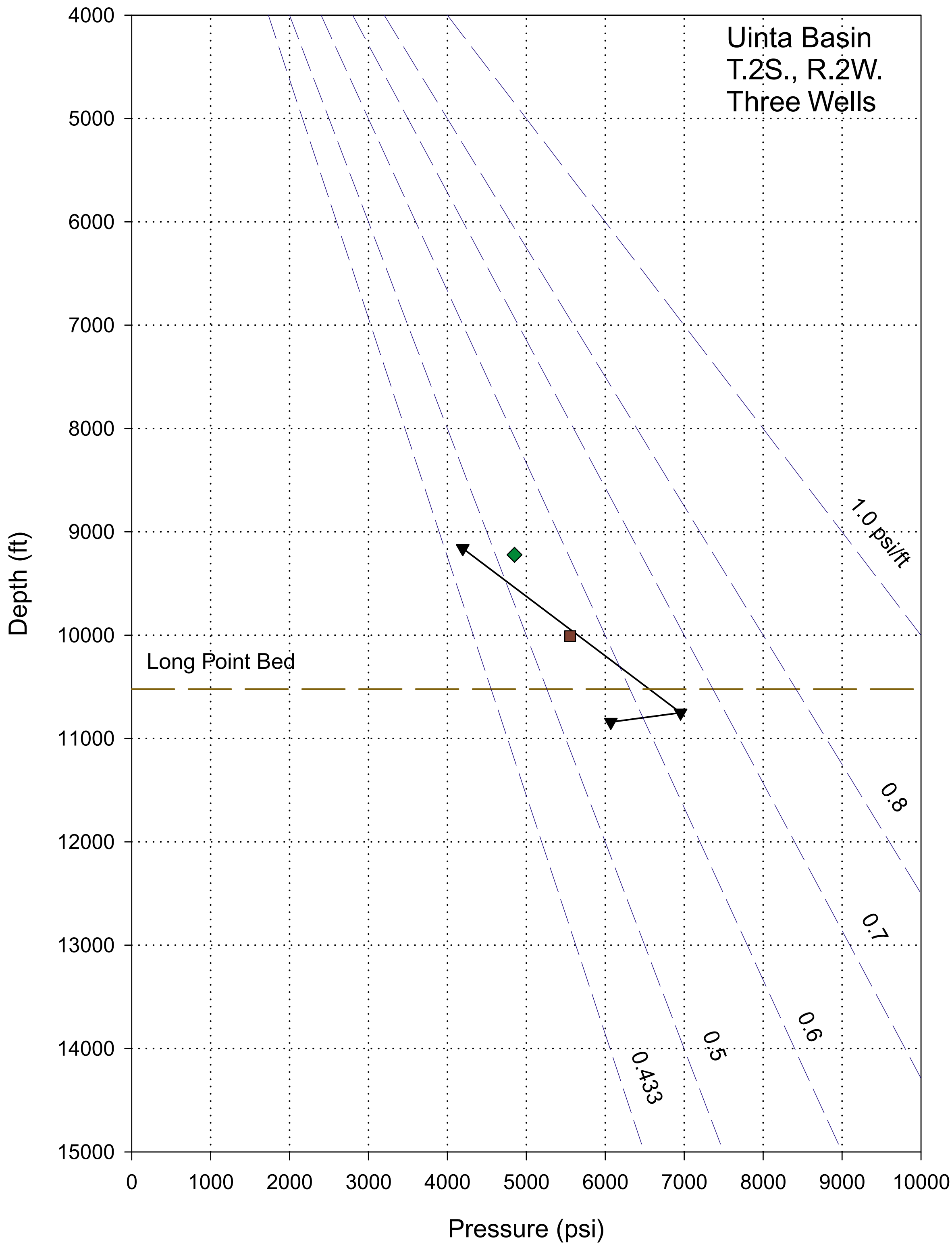

Figure 6*E*. Pressure as function of depth in T. 2 S., R. 2 W. in Altamont-Bluebell field of Uinta Basin. Each symbol represents the pressure from one drill-stem test; connected symbols show data from one well. Dashed lines show constant pressure gradient ranging from hydrostatic (0.433 psi/ft) to lithostatic (1.0 psi/ft). Depth of Long Point Bed from Johnson (1989a).

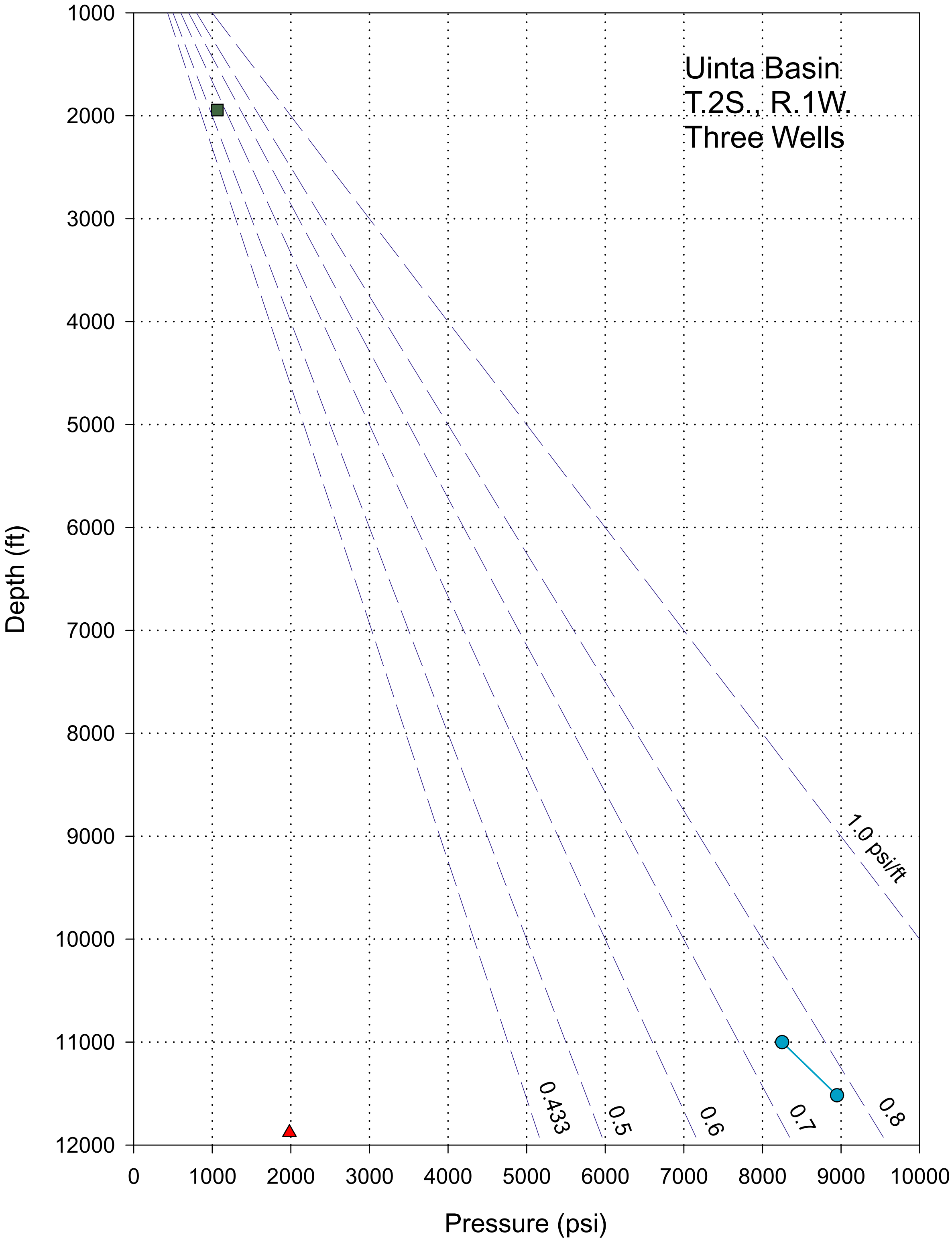

Figure 6*F*. Pressure as function of depth in T. 2 S., R. 1 W. in Altamont-Bluebell field of Uinta Basin. Each symbol represents the pressure from one drill-stem test; connected symbols show data from one well. Dashed lines show constant pressure gradient ranging from hydrostatic (0.433 psi/ft) to lithostatic (1.0 psi/ft).

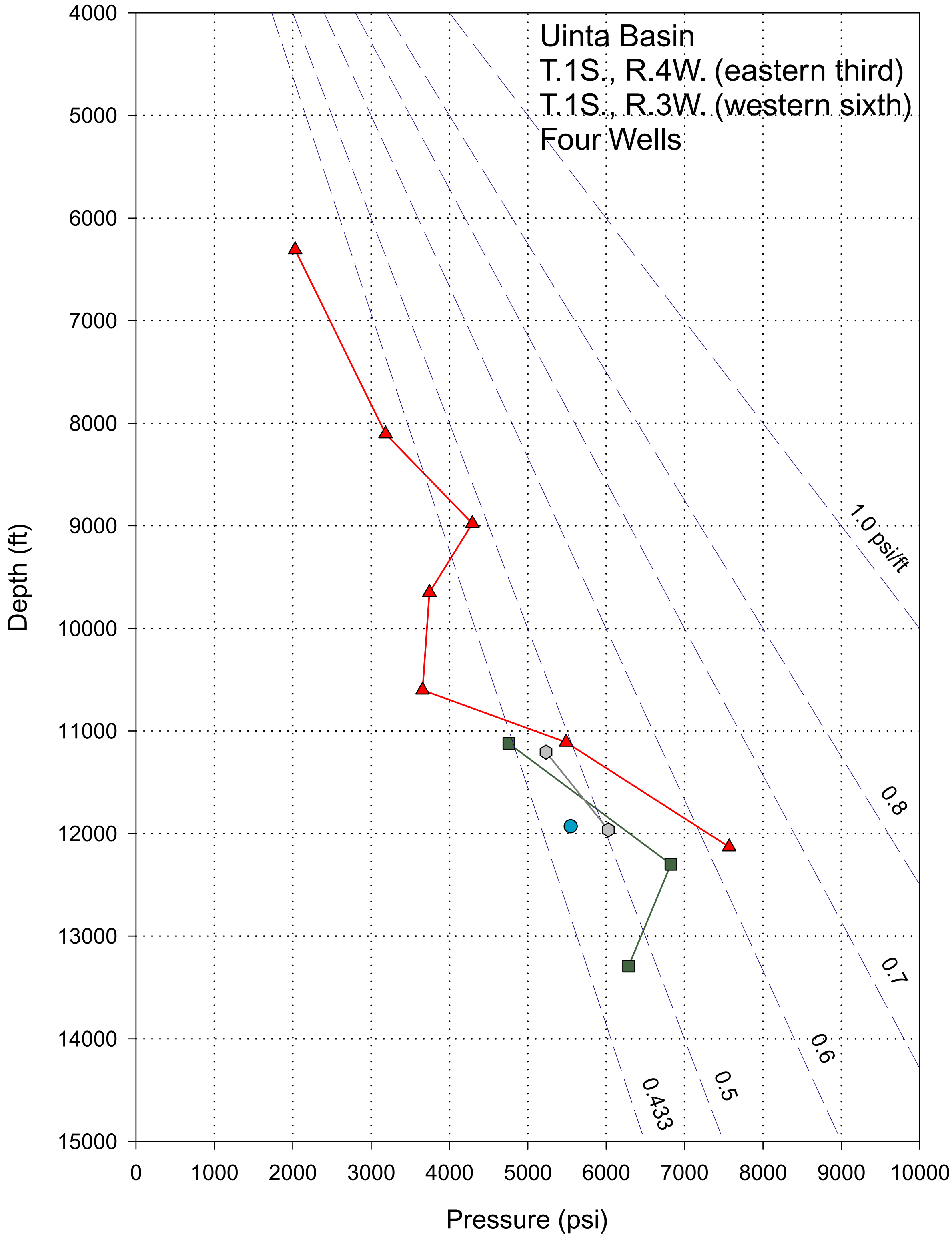

Figure 6*G*. Pressure as function of depth in T. 1 S., R. 4 W. and T. 1 S., R. 3 W. in Altamont-Bluebell field of Uinta Basin. Each symbol represents the pressure from one drill-stem test; connected symbols show data from one well. Dashed lines show constant pressure gradient ranging from hydrostatic (0.433 psi/ft) to lithostatic (1.0 psi/ft).

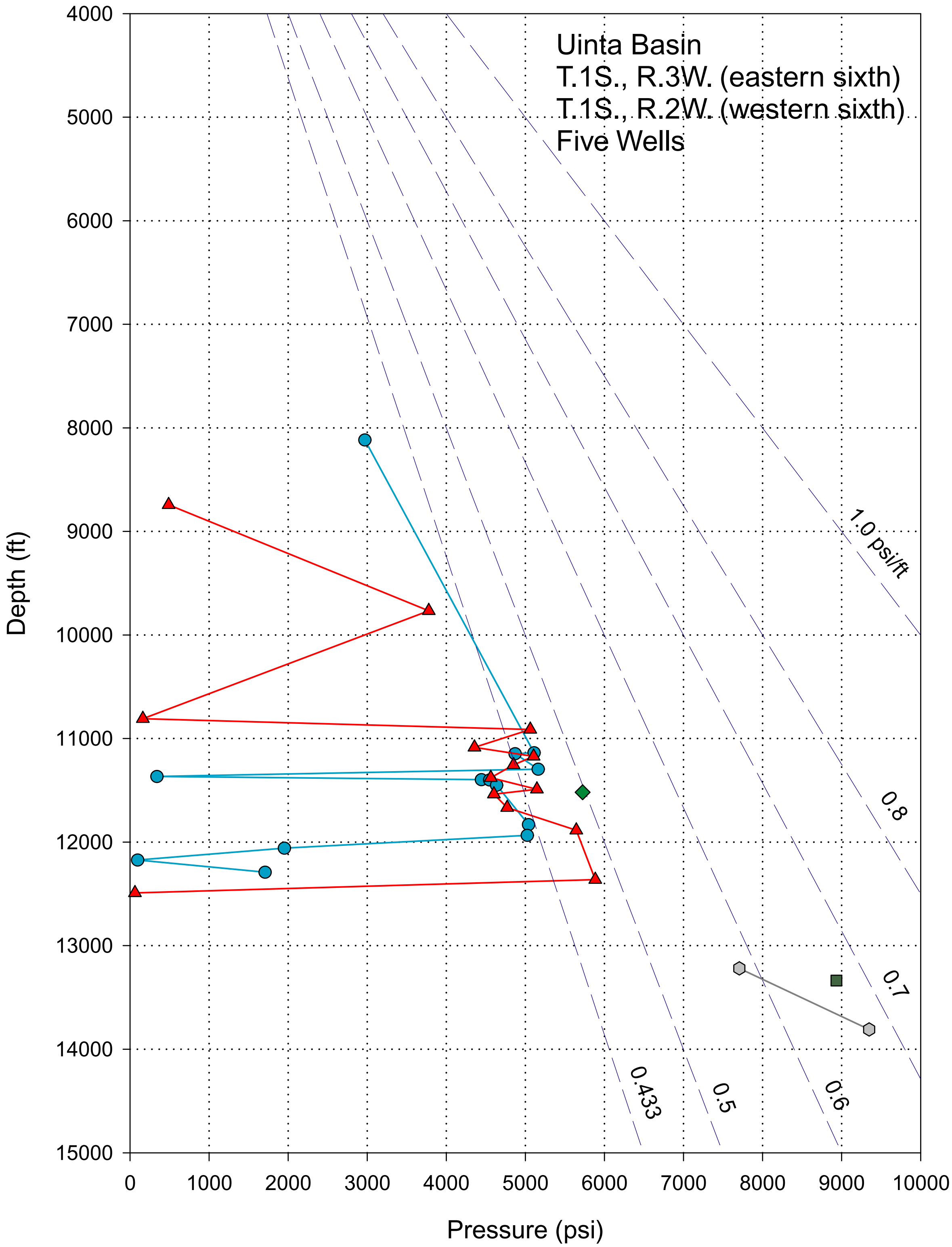

Figure 6*H*. Pressure as function of depth in T. 1 S., R. 3 W. and T. 1 S., R. 2 W. in Altamont-Bluebell field of Uinta Basin. Each symbol represents the pressure from one drill-stem test; connected symbols show data from one well. Dashed lines show constant pressure gradient ranging from hydrostatic (0.433 psi/ft) to lithostatic (1.0 psi/ft).

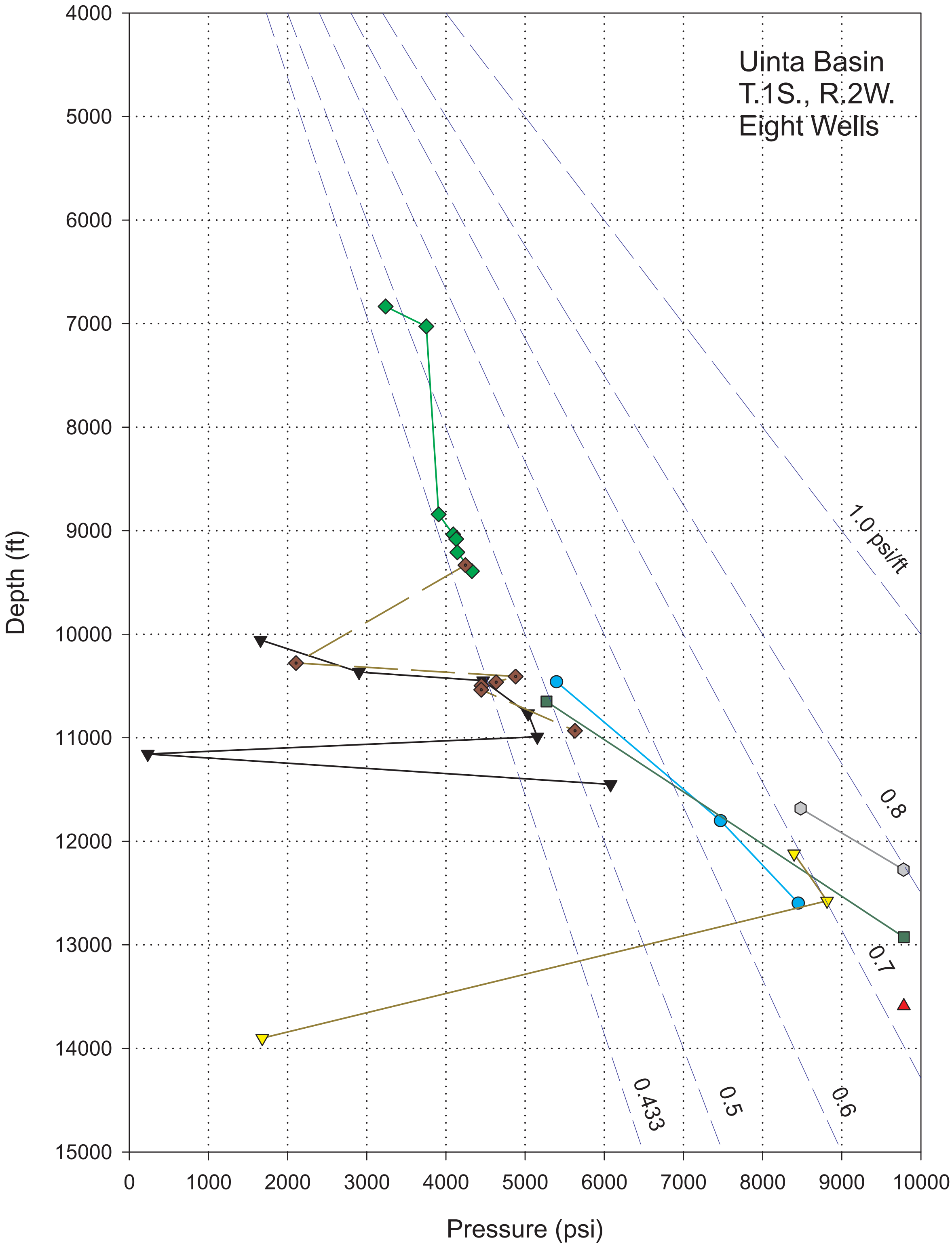

Figure 6*I*. Pressure as function of depth in T. 1 S., R. 2 W. in Altamont-Bluebell field of Uinta Basin. Each symbol represents the pressure from one drill-stem test; connected symbols show data from one well. Dashed lines show constant pressure gradient ranging from hydrostatic (0.433 psi/ft) to lithostatic (1.0 psi/ft).

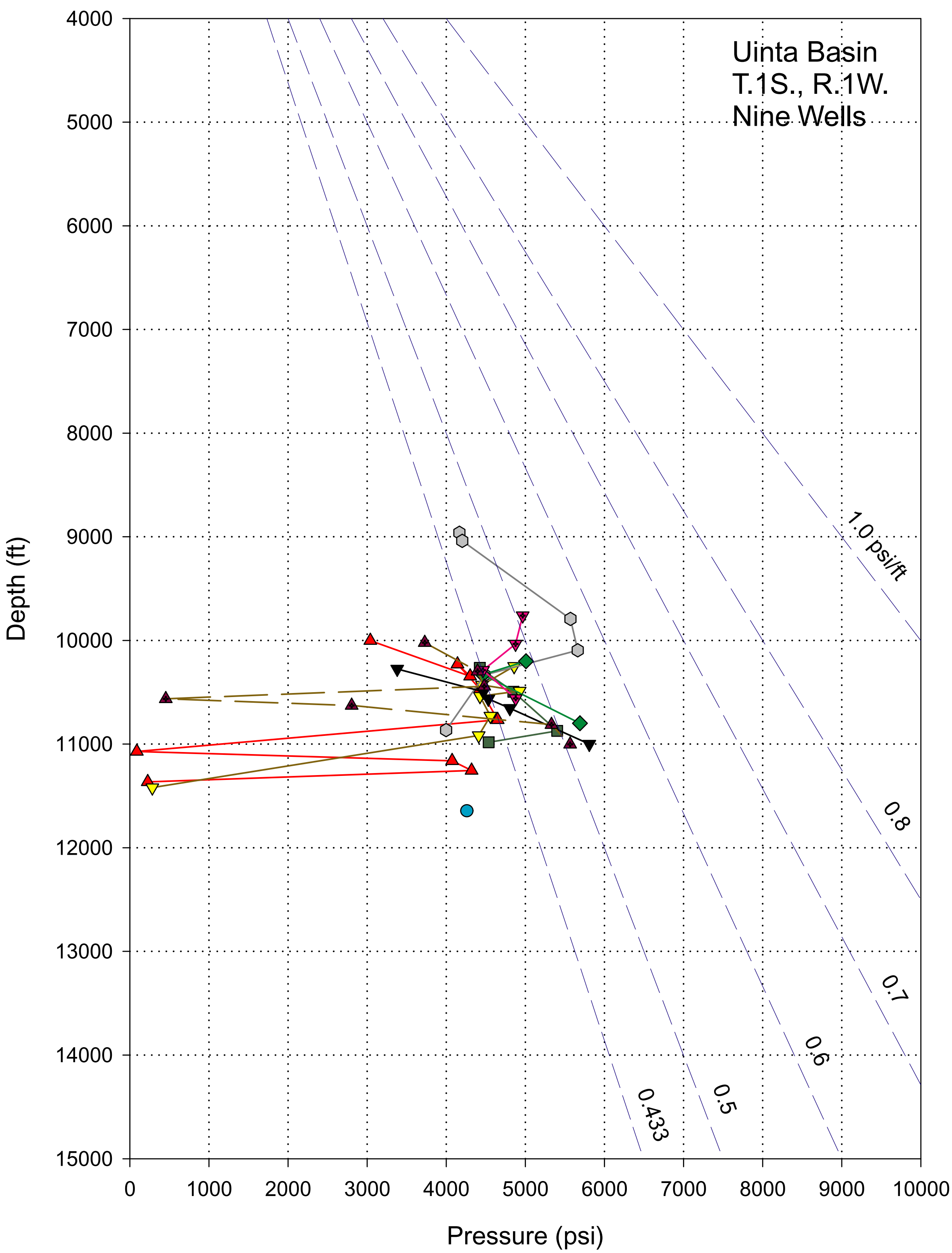

Figure 6*J*. Pressure as function of depth in T. 1 S., R. 1 W. in Altamont-Bluebell field of Uinta Basin. Each symbol represents the pressure from one drill-stem test; connected symbols show data from one well. Dashed lines show constant pressure gradient ranging from hydrostatic (0.433 psi/ft) to lithostatic (1.0 psi/ft).

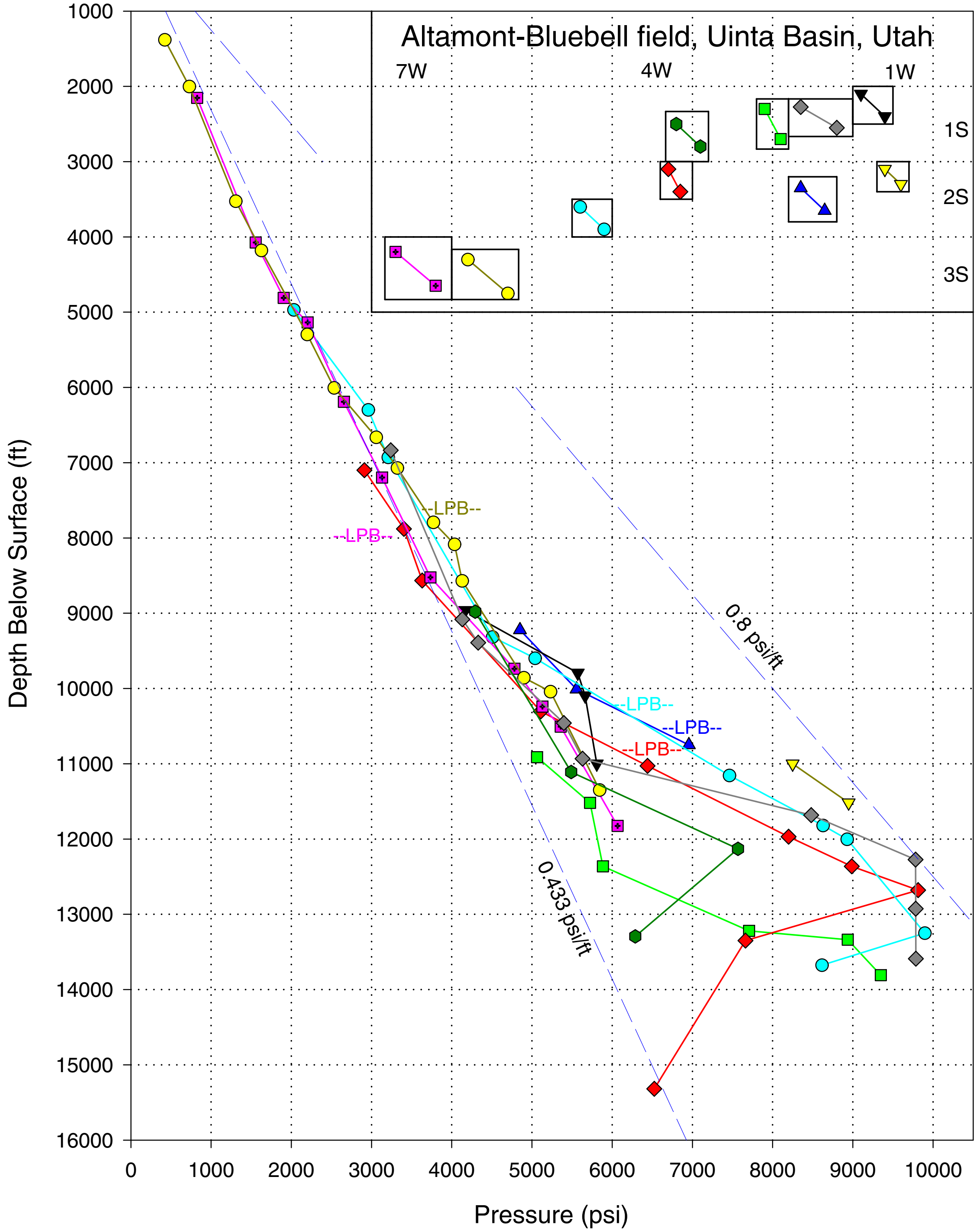

Figure 7. Apparent pressure as function of depth below surface in Altamont-Bluebell field of Uinta Basin, summarizing the 10 pressure-depth plots of figure 6*A*–*J*. Each curve joins selected points from wells within a single township, selected to represent the maximum pressure gradient. Relative locations of townships and key to curve symbols are shown in inset. "LPB" posted for five wells designates the depth of Long Point Bed, taken from Johnson (1989a).

(fig. 6*C–I*) that the nominal pressure gradient exceeds 0.6 psi/ft.

The pressures from figure 6*A–J* are abstracted and composited in figure 7. From each individual plot, pressure data were selected that outlined a high-pressure profile, ignoring those points that fall to the left of a high-pressure, right-hand "edge." For example, 10 points were selected from figure 6*D*, and 5 points were ignored; the resulting curve is represented by red diamonds in figure 7. This method permits comparison of a number of profiles that represent the tendency for overpressure to occur within a number of areas within the Altamont-Bluebell field. By omitting low-pressure excursions, the procedure omits DST data that did not reach true reservoir pressure. The same data are also presented in figures 8 and 9.

In figure 8, hydrostatic pressure has been subtracted from measured pressure, using the procedure illustrated in figure 1*C*. By removing the hydrostatic gradient, the pressure data can be viewed with greater resolution than in figure 7.

In figure 9, depth below sea level is used in place of depth below surface, thereby removing the effect of surface elevation. The differing surface elevations of individual wells cause data from different wells in figure 9 to be shifted vertically with respect to figure 7. If the pressure transition zone (or any other area-wide feature) occurred at a common depth below sea level, then the pressure curves in figure 9 would tend to coalesce. However, coalescence of curves in figure 9 improves only moderately compared to figure 7, implying that other controls such as structure or varying amounts of uplift play a greater role in determining the depth of the transition zone than does surface topography.

The procedure used to composite the data in figures 7, 8, and 9 omits those points that might represent underpressure; however, it appears unlikely that underpressure exists below a depth of 5,000 ft in the Uinta Basin. However, underpressure may exist above a depth of 5,000 ft. Pressures fall below the 0.433 psi/ft gradient in two wells within T. 3 S., R. 7 W. (fig. 6*A*) and in three wells within T. 3 S., R. 6 W. (fig. 6*B*). At depths shallower than 5,000 ft in these two areas, no pressures exceed nominal pressure gradients of 0.433 psi/ft. This consistency among wells in registering a decline in pressure to values less than hydrostatic indicates that the pressure data do represent actual "underpressure" and that fluids are isolated from the surface even at depths as shallow as 1,500 ft.

A highly overpressured zone exists in at least 7 of the 10 areas summarized in figures 7–9. Pressure data in the three remaining areas—T. 3 S., R. 7 W., T. 3 S., R. 6 W., and T. 1 S., R. 1 W.—do not extend below 5,200 ft below sea level (fig. 9), which is not deep enough to show conclusively if the highly overpressured zone is present or not.

The top of the overpressured zone is characterized by a rapid increase of pressure with depth, which can be quantified in terms of the local pressure gradient (fig. 1*A*). In the 1 Shell Murdock well in T. 2 S., R. 5 W. (fig. 6*C*), the local pressure gradient is 1.62 psi/ft between 9,600 and 12,000 ft. In the 1-11-B4 Shell Brotherson well in T. 2 S., R. 4 W. (fig. 6*D*), the local pressure gradient is 1.88 psi/ft between 10,300 and 12,360 ft. Local pressure gradients greater than 1.0 psi/ft within vertical intervals of several thousand feet were also found in Tertiary oil fields in south Texas by Leftwich and Engelder (1994) and Engelder and Leftwich (1997). Transition zones with high local pressure gradients are often interpreted as pressure seals (Bradley and Powley, 1994; Hunt and others, 1998).

In at least four townships (fig. 6*C*, *D*, *F*, *H*, and fig. 7), the pressure declines at depth to values less than the maximum pressures, giving the appearance of a zone of pressure maximum approximately 2,000 ft thick. Given the probable underrepresentation of actual pressure from DSTs, it cannot be stated with complete confidence that the pressure downturn is valid. But if it is, then the zone of maximum pressure occurs at a depth between 12,000 and 14,000 ft subsurface, equivalent to a depth range of 6,000–8,000 ft below sea level.

Lucas and Drexler (1976) mapped the distribution of overpressure in the Altamont-Bluebell field in the Uinta Basin (see fig. 18 in chapter 5 by Dubiel, this CD-ROM). Lucas and Drexler based their map upon mud weights, borehole pressure measurements, and DST pressures. Their contours of pressure gradient represent all Tertiary data, without segregation by depth or formation. Their mapping shows a maximum observed reservoir pressure gradient exceeding 0.7 psi/ft within an area about 30 mi in east-west extent and 15 mi north-south. Within this area, the gradient slightly exceeds 0.8 psi/ft in two areas. The area of overpressure mapped by Lucas and Drexler coincides with the townships of figure 5 showing overpressure, but their contours indicate generally higher pressure gradients than the highest values shown in figure 5. It is possible that the Lucas and Drexler data set is more highly populated than the data set presented here, thereby giving a better representation of the state of subsurface fluid pressure.

Eastern Part of Uinta Basin

For purposes of this discussion, the eastern part of the Uinta Basin is considered to include all townships east of and including R. 18 E. (figs. 2 and 5). The distributions of all pressure data for six representative townships are shown in figure 10*A–F*, whereas pressure gradients greater than 0.4 are shown in figure 5.

Occurrences of overpressure in the eastern part of the Uinta Basin appear to be moderate and sporadic (fig. 5). Many of the DSTs run in 12 wells of T 11 S., R. 23 E. (fig. 10*F*) show that pressure gradients reach but do not exceed 0.5 psi/ft, indicating that many intervals are moderately overpressured but not significantly overpressured. Data from other townships (fig. 10*A–E*) show pressure gradients in excess of 0.5 psi/ft, but the data are too spotty to make any judgments about spatial trends. Overall, there is no indication of a sudden increase in pressure with increasing depth as exists across much of the Altamont-Bluebell field.

The distribution of normally pressured and overpressured measurements in the eastern Uinta Basin is given in table 1. A

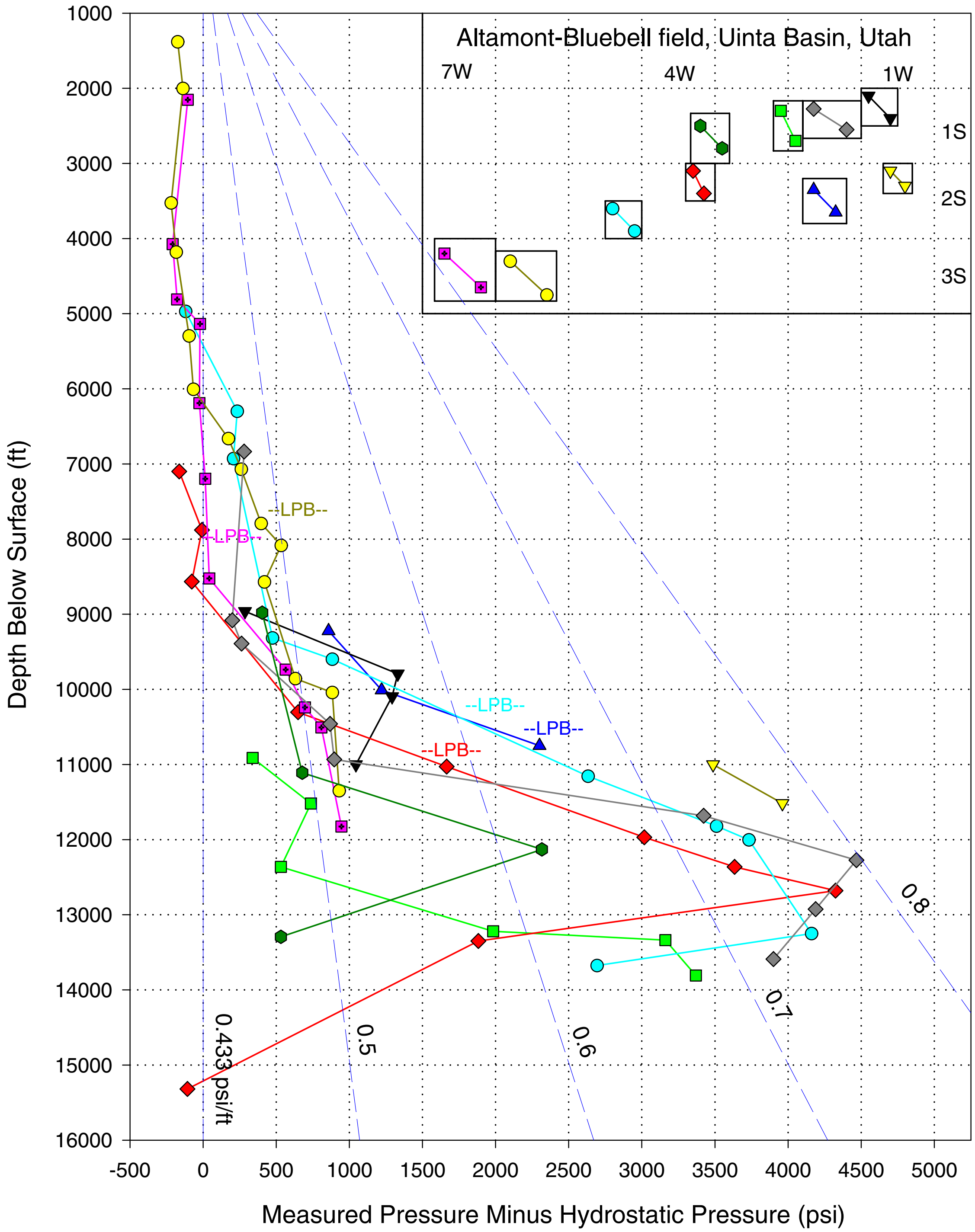

Figure 8. Differential pressure as function of depth below surface in Altamont-Bluebell field of Uinta Basin. Differential pressure is equal to measured apparent pressure minus 0.433 times depth. The vertical zero line represents hydrostatic pressure with a gradient of 0.433 psi/ft. Each curve joins selected points from wells within a single township, selected to represent the maximum pressure gradient. Relative locations of townships and key to curve symbols are shown in inset. "LPB" posted for five wells designates the depth of Long Point Bed, taken from Johnson (1989a).

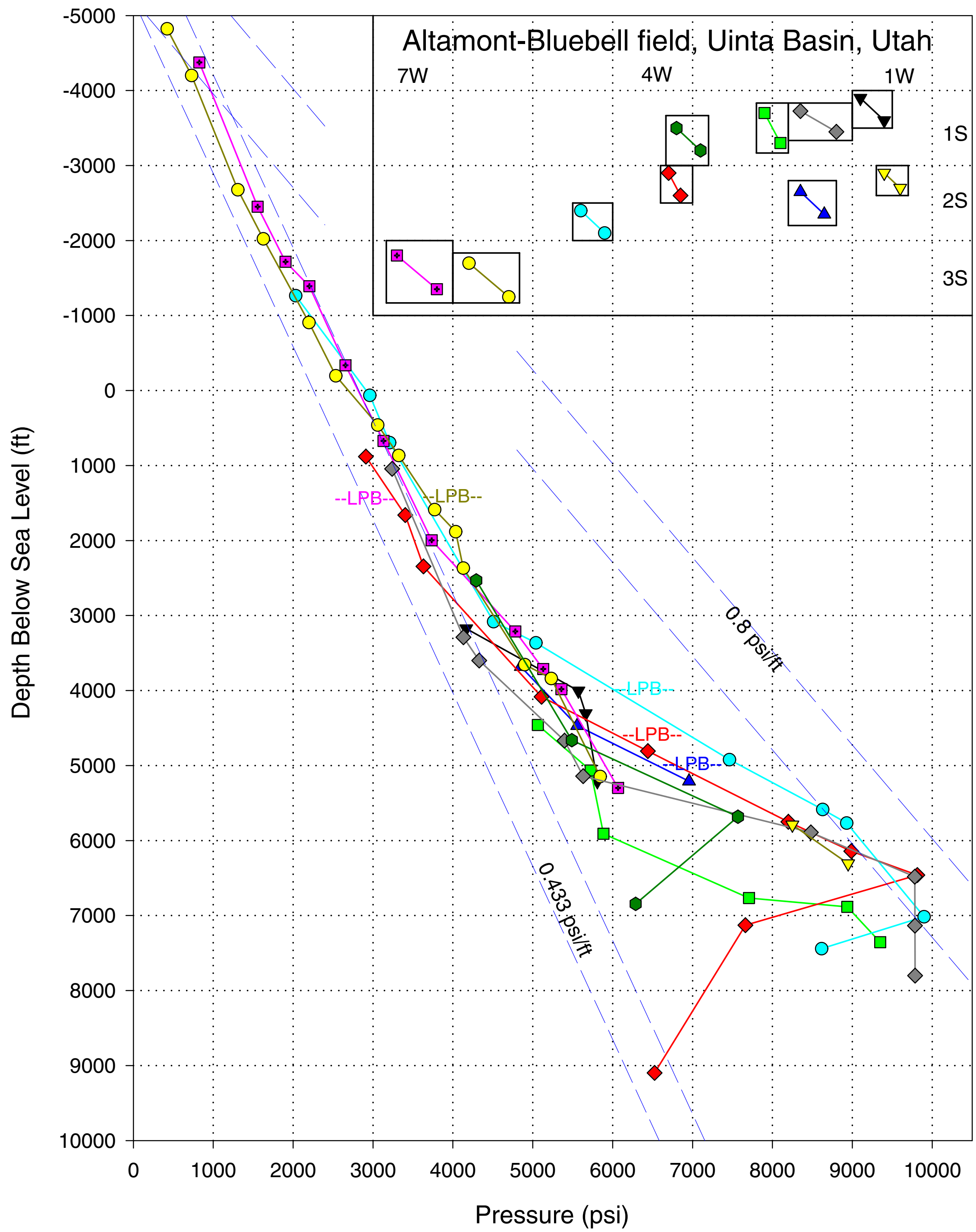

Figure 9. Apparent pressure as function of depth below sea level in Altamont-Bluebell field of Uinta Basin. Each curve joins selected points from wells within a single township, selected to represent the maximum pressure gradient. Relative locations of townships and key to curve symbols are shown in inset. "LPB" posted for five wells designates the depth of Long Point Bed, taken from Johnson (1989a). Pressure gradients are here represented by a spread of parallel lines with bounds shown for 0.433 and 0.80 psi/ft.

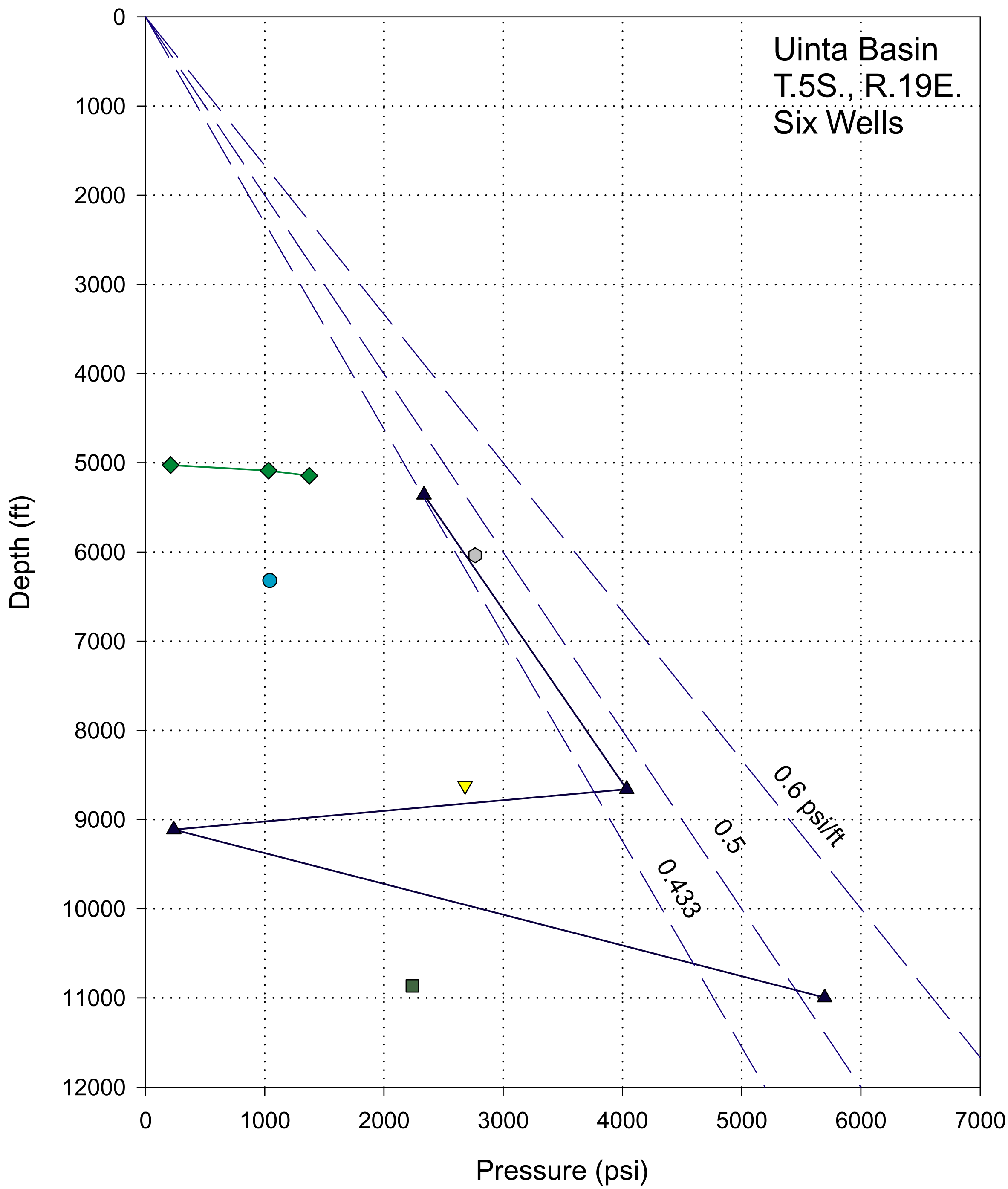

Figure 10*A*. Apparent pressure as function of depth in T. 5 S., R. 19 E. of Uinta Basin. Each symbol represents the pressure from one drill-stem test; connected symbols show data from one well. All tests were run in Tertiary rocks.

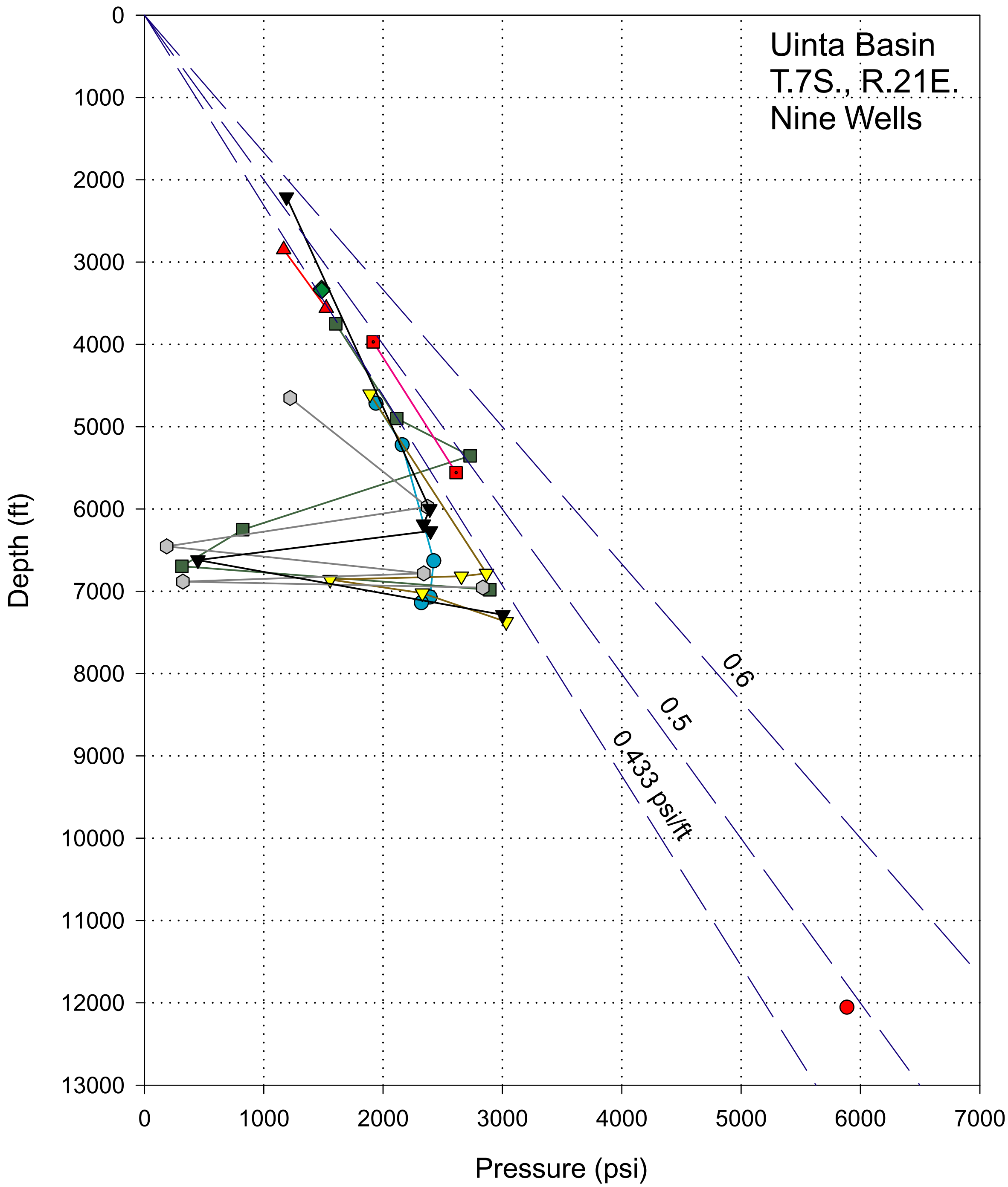

Figure 10*B*. Apparent pressure as function of depth in T. 7 S., R. 21 E. of Uinta Basin. Each symbol represents the pressure from one drill-stem test; connected symbols show data from one well. All tests were run in Tertiary rocks except the single data point at 12,000 ft.

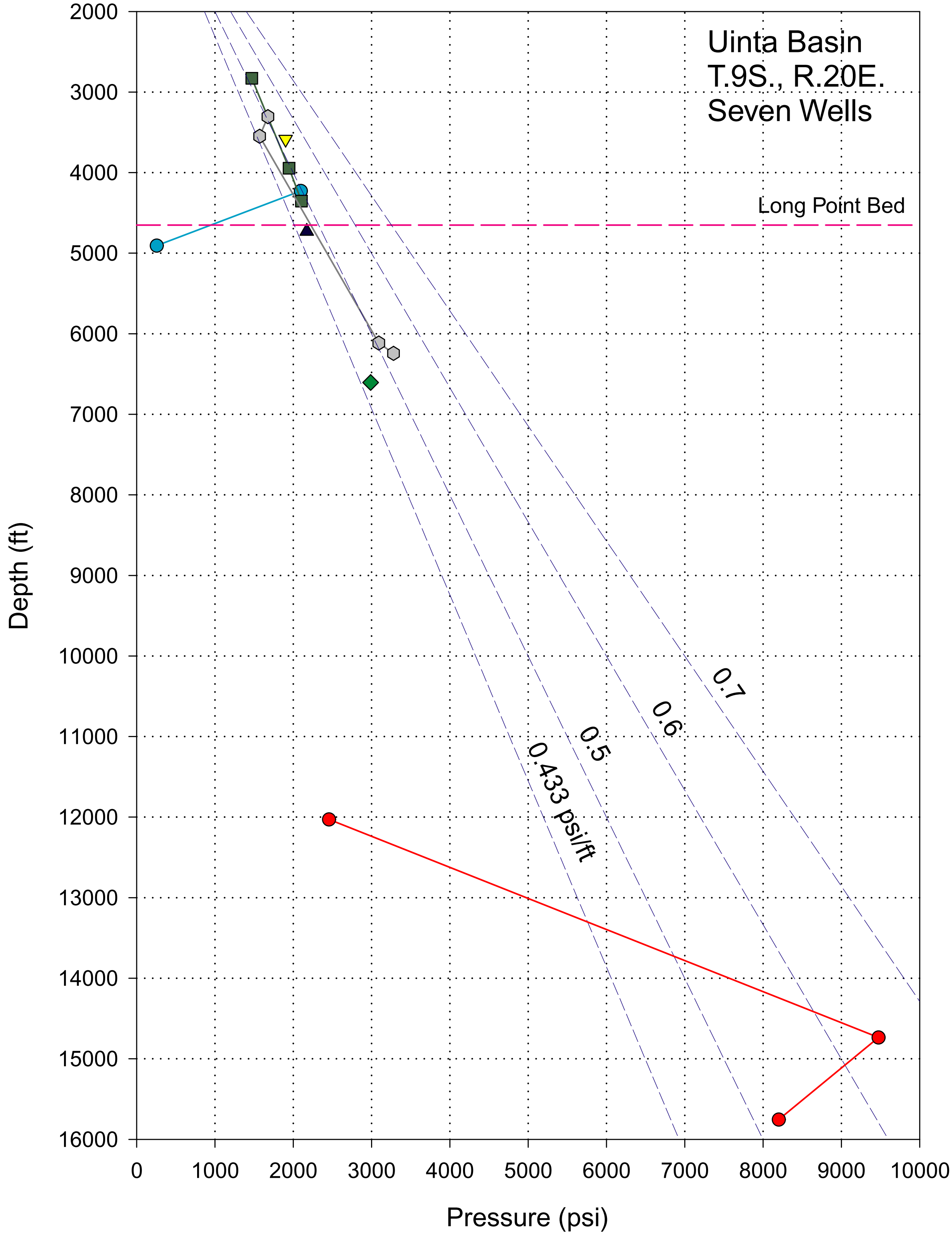

Figure 10*C*. Apparent pressure as function of depth in T. 9 S., R. 20 E. of Uinta Basin. Each symbol represents the pressure from one drill-stem test; connected symbols show data from one well. All tests above 7,000 ft were run in Tertiary rocks; three tests below 12,000 ft are in Cretaceous rocks.

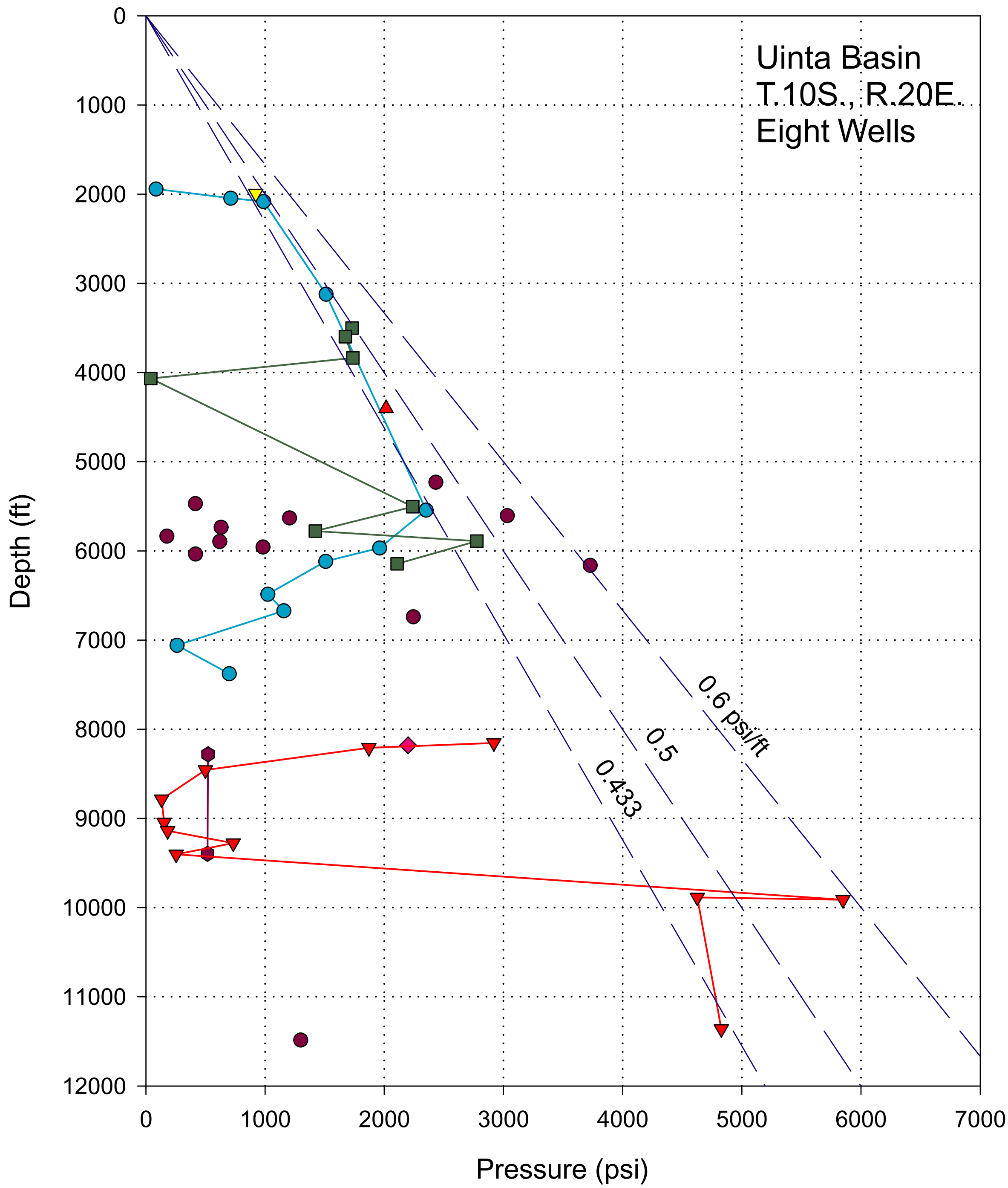

Figure 10*D*. Apparent pressure as function of depth in T. 10 S., R. 20 E. of Uinta Basin. Each symbol represents the pressure from one drill-stem test; connected symbols show data from one well. All tests below 8,000 ft were run in Cretaceous rocks.

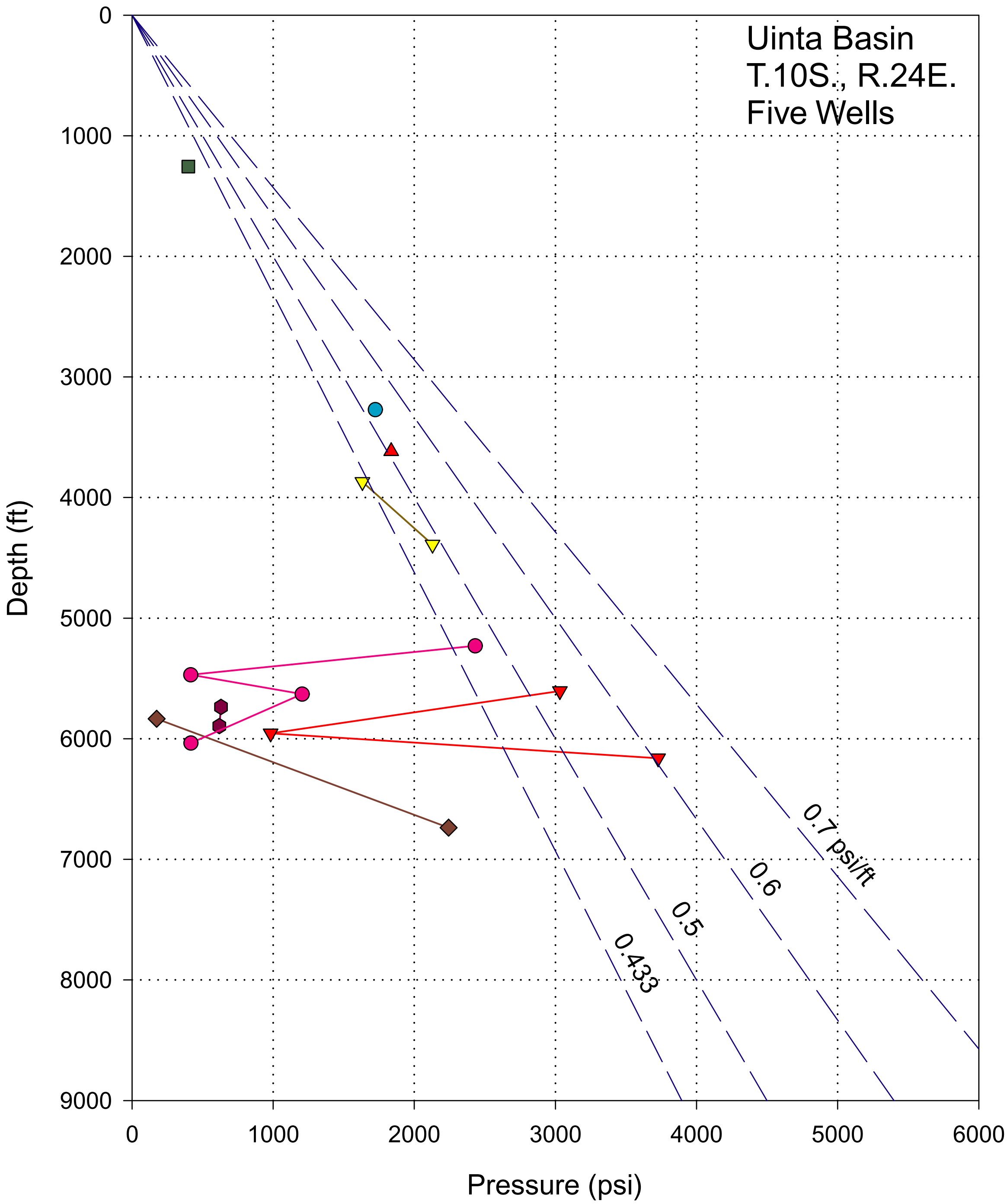

Figure 10*E*. Apparent pressure as function of depth in T. 10 S., R. 24 E. of Uinta Basin. Each symbol represents the pressure from one drill-stem test; connected symbols show data from one well. All tests below 5,000 ft were run in Cretaceous rocks.

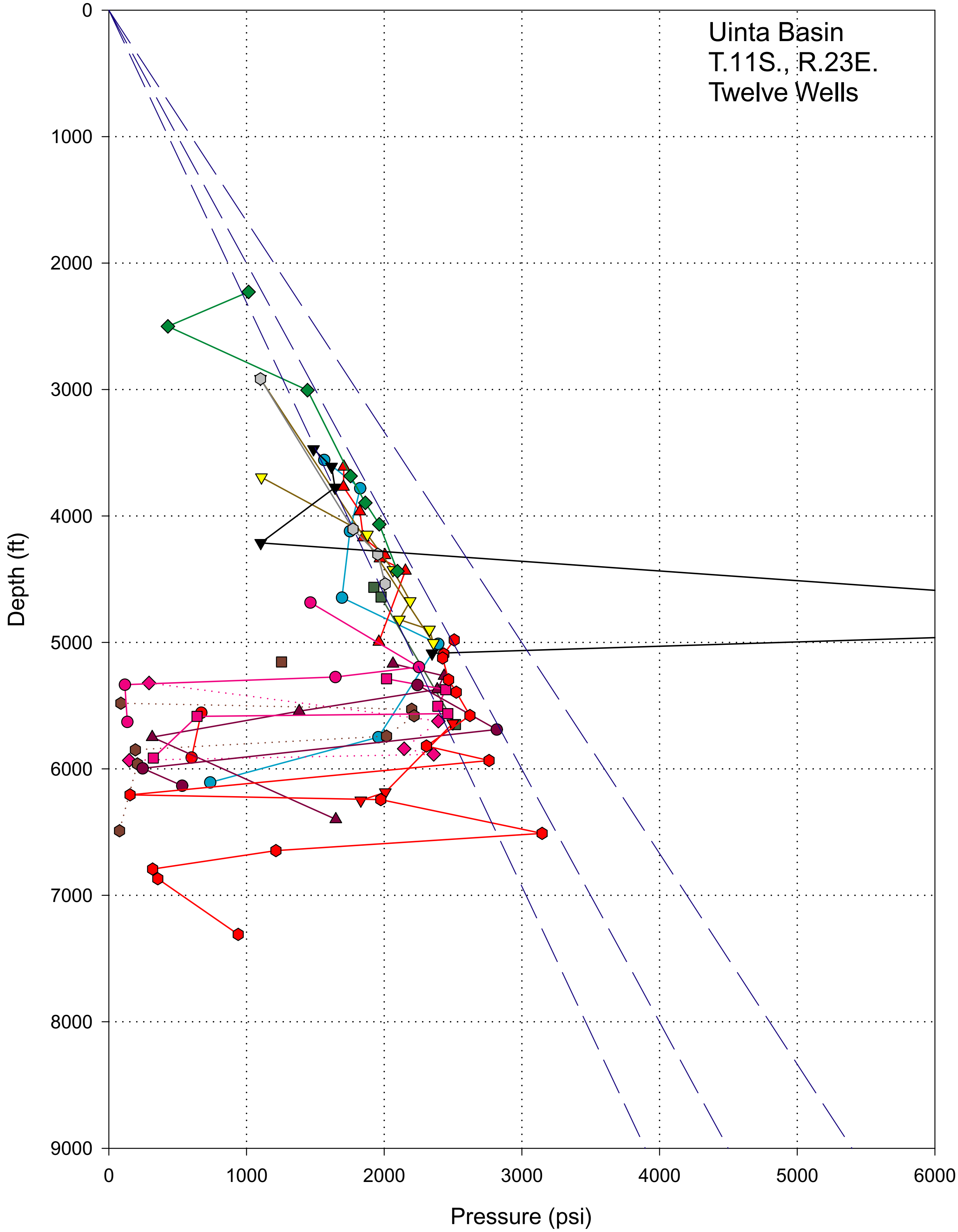

Figure 10*F*. Apparent pressure as function of depth in T. 11 S., R. 23 E. of Uinta Basin. Each symbol represents the pressure from one drill-stem test; connected symbols show data from one well. (One off-scale measurement of 9,379 psi (2.075 psi/ft) is probably erroneous; tests marked with red, brown, and purple symbols, most of which lie below 5,000 ft, were run in Cretaceous rocks; intermingling of Tertiary and Cretaceous data points is due to depth overlap among different wells and mislabeling of rock units.)

Table 1. Number of pressure measurements in eastern Uinta Basin (R. 18 E. to R. 25 E. and T. 5 S. to T. 15 S.).

Pressure Gradient (psi/ft)	Tertiary	Cretaceous
0.433–0.46	87	19
0.46–0.50	108	19
0.50–0.60	34	16
>0.60	0	3

higher fraction of measurements in Cretaceous rocks exceeds 0.5 psi/ft than in Tertiary rocks; this skewness may indicate that the Cretaceous rocks are more consistently overpressured than the Tertiary rocks.

Only three measurements in Cretaceous rocks exceeded 0.60 psi/ft: a value of 0.62 at 4,668 ft in the Mesaverde Formation in sec. 8, T. 11 S., R. 24 E., a value of 1.101 (probably erroneous) at 7,450 ft in the Niobrara Formation in sec. 4, T. 15 S., R. 23 E., and a value of 0.646 at 14,666 ft in the Castlegate Sandstone, also in sec. 4, T. 15 S., R. 23 E. (this latter township lies south of the southern boundary of the area of figs. 2 and 5). Overpressuring is detected as deep as 15,700 ft in Cretaceous rocks in T. 9 S., R. 20 E. (fig. 10*C*).

Evidence for underpressured zones in the eastern Uinta Basin is spotty at best (figs. 5 and 10). Pressure values less than hydrostatic are frequently intermingled with values of 0.433 psi/ft and greater. Exceptions occur, such as the zone from 6,800 to 7,300 ft in T. 7 S., R. 21 E. (fig. 10*B*), where six measurements fall between 0.37 and 0.433 psi/ft and there are no DSTs with higher pressures. This zone could be underpressured.

Piceance Basin

Pressure data for the Piceance Basin are presented in figures 11 and 12; map locations of townships and wells are shown in figure 3. Three symbols are used to designate pressure measurements in three age groupings of rock formations. The 50 cyan squares represent measurements from the Dakota Formation (33 measurements) and other Cretaceous formations underlying the Mesaverde Group, including the Mancos Shale (7 samples). The 58 red triangles represent measurements from the Mesaverde Group, as well as the Rollins, Corcoran, and Cozzette Sandstone Members of the Iles Formation. The 18 black “plus” symbols represent measurements from Tertiary strata.

Pressure data from the Piceance Basin show less evidence of widespread overpressured intervals than do the data from the Uinta Basin. The highest pressure gradients were detected in well tests in the MWX-1 well in R. 94 W., T. 6 S. (fig. 12; also see chapter 15 by Nelson, this CD-ROM). As can be seen in figures 11 and 12, pressure gradients do not exceed 0.6 psi/ft in any other wells in the Piceance Basin, at least not in the pre-1985 data compilation discussed here (two high-pressure exceptions occur at shallow depths in T. 5 S., R. 102 W. in figure 11, and in T. 8 S., R. 101 W. in figure 12). The detection of pressure gradients in experimental well MWX-1 that are greater than any pressure gradients measured in nearby wells from DSTs can be attributed in large part to the extreme care taken in MWX-1 to establish pressure communication with the formation and to allow sufficient time for pressure to build in low-permeability formations. The difficulty in obtaining reliable formation pressure data in the Mesaverde Group in the Piceance Basin has been noted by Johnson (1989b, p. E31). This difficulty notwithstanding, an overpressured zone within the Mesaverde Group, determined partly from mud weights, is mapped as a teardrop-shaped area extending from T. 6 S., R. 94 W. on the northwest to T. 8 S., R. 92 W. on the southeast (fig. 8 of Wilson and others, 1998).

Data in figures 11 and 12 provide little or no information on pressures below the Mesaverde Group within the center of the Piceance Basin. However, normal to slight overpressuring is shown within the Dakota Formation where it is penetrated at depths within 5,000 ft of the surface on the Douglas Creek arch (fig. 11).

Summary

It is now well established that zones of abnormal pressure (both underpressure and overpressure) are associated with hydrocarbon accumulations, particularly in continuous accumulations occurring in the Rocky Mountain basins. Checkerboard plots of DST pressures (figs. 5, 11, and 12) can be used to check the adequacy of DST pressure data in a basin and to examine lateral and vertical trends in formation pressure.

Overpressuring occurs throughout much of the Uinta Basin (fig. 5). Significant overpressuring (0.5<pressure gradient<0.8 psi/ft) is found throughout the Altamont-Bluebell field at depths ranging from 10,000 to 13,000 ft, equivalent to 5,000–8,000 ft below sea level. Limited data indicate that the pressure gradient declines at depths greater than 13,000 ft.

Throughout the eastern Uinta Basin, moderate overpressure (0.46<pressure gradient<0.5 psi/ft) occurs commonly, with local evidence of significant overpressuring. Pressure gradients greater than 0.6 psi/ft are rare. Most tests were run at depths shallower than 7,000 ft below surface, but three tests measured significant overpressure (>0.5 psi/ft) in Cretaceous rocks at depths greater than 14,000 ft below surface.

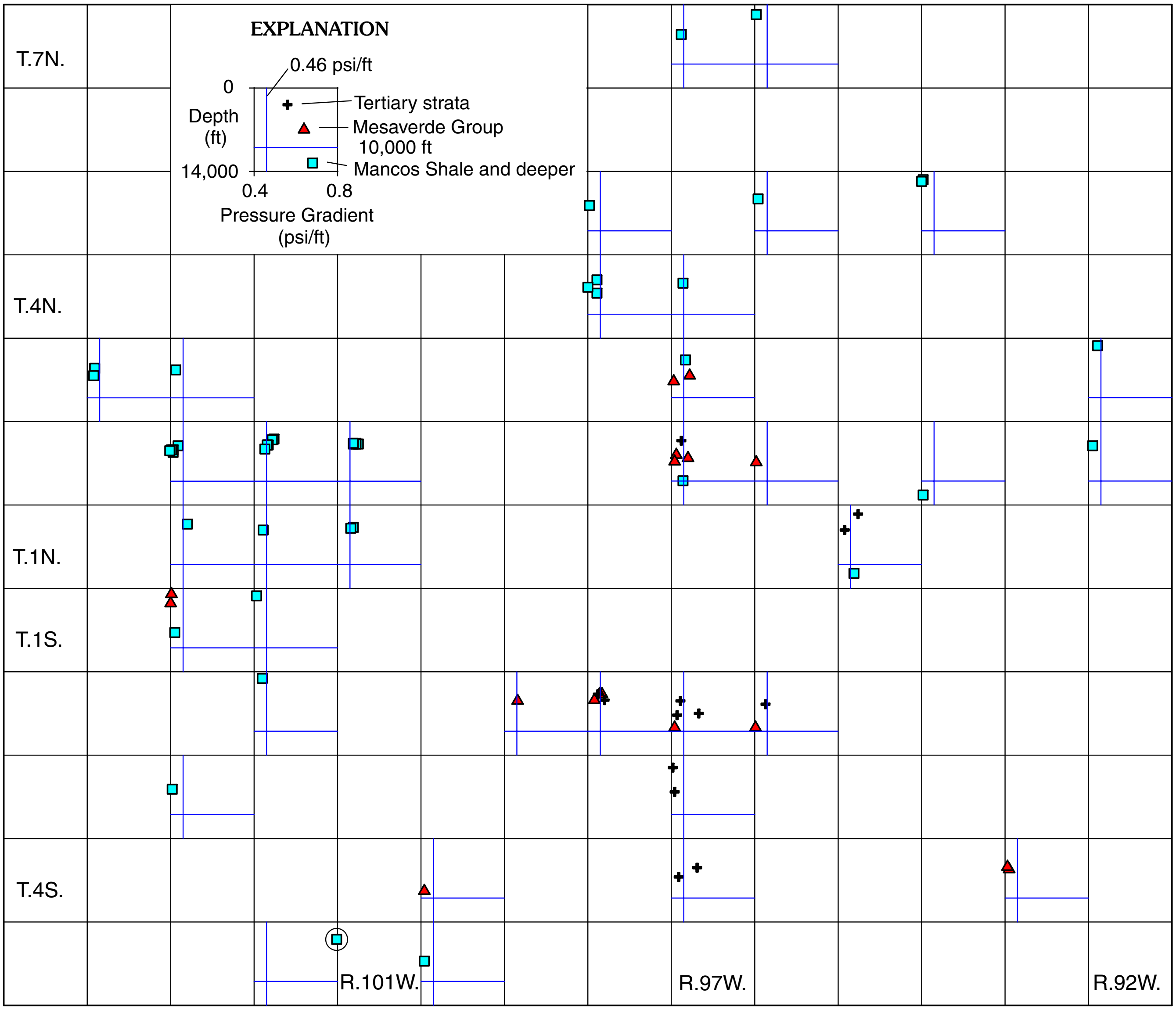

Figure 11. Apparent pressure gradient as function of depth in northern Piceance Basin. Each square shows all drill-stem tests within a township recording an apparent pressure gradient greater than 0.4 psi/ft. Within a square, pressure gradients range from 0.4 to 0.8 psi/ft and depth ranges from 0 to 14,000 ft below surface. A circled point in T. 5 S., R. 102 W. represents a measurement at 2,935 ft with a pressure gradient (off scale) of 1.39 psi/ft. Vertical blue line shows a reference gradient of 0.46 psi/ft and horizontal blue line shows a depth reference of 10,000 ft.

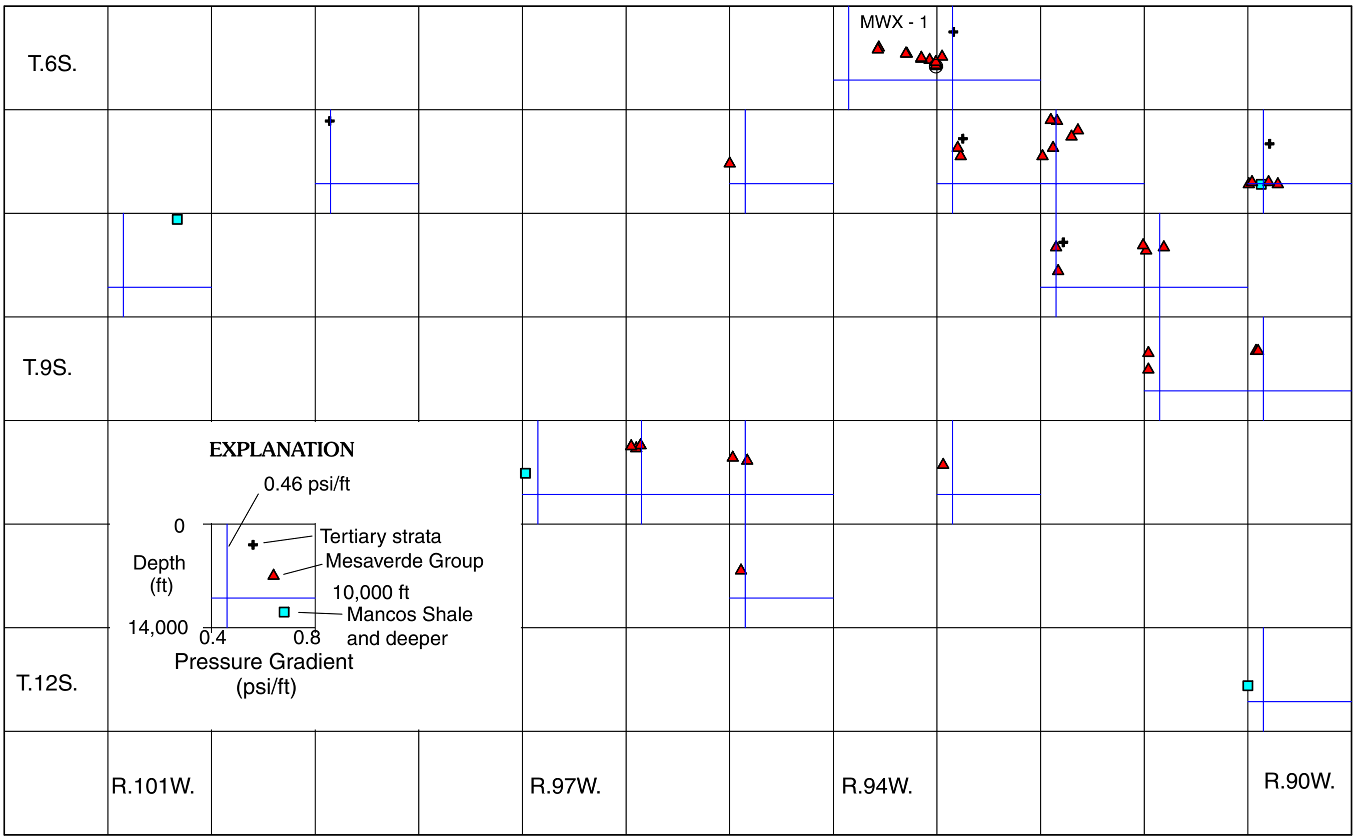

Figure 12. Apparent pressure gradient as function of depth in southern Piceance Basin. Each square shows all drill-stem tests within a township recording an apparent pressure gradient greater than 0.4 psi/ft. Within a square, pressure gradients range from 0.4 to 0.8 psi/ft and depth ranges from 0 to 14,000 ft below surface. A circled point in T. 6 S., R. 94 W. represents a measurement at 8,110 ft with a pressure gradient (slightly off scale) of 0.825 psi/ft. Vertical blue line shows a reference gradient of 0.46 psi/ft and horizontal blue line shows a depth reference of 10,000 ft.

In the Piceance Basin, the spatial density of pressure tests and the pressures measured are both less than in the Uinta Basin. Pressures measured in well tests in well MWX-1 are higher than pressures measured in nearby wells and also greater than those measured anywhere else in the basin, raising the possibility that DSTs provide inadequate measurements of pressure in Cretaceous rocks in the Piceance Basin.

In the Uinta Basin, the apparent pressure gradients from DSTs (that is, initial or final pressures) were compared with actual pressure gradients that had been extrapolated to reservoir pressure using the Horner method. In a sample of 34 extrapolated DSTs, it was found that actual values exceeded apparent ones in 32 percent of cases by a range of 0.02–0.15 psi/ft, with an average difference of 0.06 psi/ft. Although a user of the data should remain aware of this difference, the general agreement between final and extrapolated pressure demonstrates that DSTs provide useful measurements of fluid pressure within the Uinta Basin.

Acknowledgments

C.W. Spencer designed a compilation of DST data and R.C. Obuch recovered the files from magnetic tape. Reviews by V.F. Nuccio, R.F. Dubiel, and C.W. Spencer and a comment by J.K. Pitman led to improvements in the manuscript.

References Cited

Bradley, J.S., and Powley, D.E., 1994, Pressure compartments in sedimentary basins, a review, *in* Ortoleva, P.J., ed., Basin compartments and seals: American Association of Petroleum Geologists Memoir 61, p. 3–26.

Collins, A.G., 1992, Properties of produced waters, Chapter 24 *in* Bradley, H.B., ed., Petroleum engineering handbook: Society of Petroleum Engineers, Richardson, Texas, 23 p.

Engelder, T., and Leftwich, J.T., Jr., 1997, A pore-pressure limit in overpressured South Texas oil and gas fields, 1997, *in* Surdam, R.C., ed., Seals, traps, and petroleum systems: American Association of Petroleum Geologists Memoir 67, p. 255–268.

Holm, G.M., 1998, Distribution and origin of overpressure in the Central Graben of the North Sea, *in* Law, B.E., Ulmishek, G.F., and Slavin, V.I., eds., Abnormal pressures in hydrocarbon environments: American Association of Petroleum Geologists Memoir 70, p. 123–144.

Hunt, J.M., Whelan, J.K., Eglinton, L.B., and Cathles, L.M., III, 1998, Relation of shale porosities, gas generation, and compaction to deep overpressures in the U.S. Gulf Coast, *in* Law, B.E., Ulmishek, G.F., and Slavin, V.I., eds., Abnormal pressures in hydrocarbon environments: American Association of Petroleum Geologists Memoir 70, p. 87–104.

Johnson, R.C., 1989a, Detailed cross section correlating the Upper Cretaceous and lower Tertiary rocks between the Uinta basin of eastern Utah and western Colorado and the Piceance basin of western Colorado: U.S. Geological Survey Miscellaneous Investigations Map Series I–1974, 2 sheets.

———1989b, Geologic history and hydrocarbon potential of Late Cretaceous-age, low-permeability reservoirs, Piceance Basin, western Colorado: U.S. Geological Survey Bulletin 1787–E, 51 p.

Law, B.E., and Spencer, C.W., 1998, Abnormal pressure in hydrocarbon environments, *in* Law, B.E., Ulmishek, G.F., and Slavin, V.I., eds., Abnormal pressures in hydrocarbon environments: American Association of Petroleum Geologists Memoir 70, p. 1–11.

Leftwich, J.T., Jr., and Engelder, T., 1994, The characteristics of geopressure profiles in the Gulf of Mexico Basin, *in* Ortoleva, P.J., ed., Basin compartments and seals: American Association of Petroleum Geologists Memoir 61, p. 119–130.

Lucas, P.T., and Drexler, J.M., 1976, Altamont-Bluebell—A major, naturally fractured stratigraphic trap, Uinta Basin, Utah, *in* North American oil and gas fields: American Association of Petroleum Geologists Memoir 24, p. 121–135.

Spencer, C.W., 1987, Hydrocarbon generation as a mechanism for overpressuring in Rocky Mountain region: American Association of Petroleum Geologists Bulletin, v. 71, no. 4, p. 368–388.

———1994, Abnormal formation pressures caused by hydrocarbon generation, Chapter 12 *in* Fertl, W.H., Chapman, R.E., and Hotz, R.F., eds., Studies in abnormal pressures: Developments in Petroleum Science, 38, Elsevier Press, p. 343–375.

Wesley, J.B., Wandrey, C.J., and Fouch, T.D., 1990, Principal drill stem test database (UBDST) and documentation—Analysis of Uinta Basin, Utah, gas-bearing Cretaceous and Tertiary strata: U.S. Department of Energy contract no. DE-AI21-83MC20422, 18 p.

Wilson, M.S., Gunneson, B.G., Peterson, K., Honore, R., and Laughland, M.M., 1998, Abnormal pressures encountered in a deep wildcat well, southern Piceance Basin, Colorado, *in* Law, B.E., Ulmishek, G.F., and Slavin, V.I., eds., Abnormal pressures in hydrocarbon environments: American Association of Petroleum Geologists Memoir 70, p. 195–214.

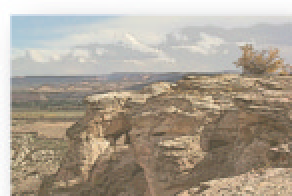

Click here to return to
Volume Title Page